IMPACT OF LAND COVER AND SOIL CONSERVATION ON SOIL EROSION RATES IN THE TIKUR WOHA CATCHMENT, ETHIOPIA

Jelle Degen

Universiteit Utrecht

IMPACT OF LAND COVER AND SOIL CONSERVATION ON SOIL EROSION RATES IN THE TIKUR WOHA CATCHMENT, ETHIOPIA

Master Thesis

Author: Jelle Degen

Student number: 5563658

E-mail: j.w.a.degen@students.uu.nl

First supervisor: Elisabeth Addink
Second supervisor: Marjolein Vogels

MSc Programme: Earth Surface and Water

Track: Natural hazards and earth observations

Faculty of Geosciences

Department of Physical Geography Utrecht University

Universiteit Utrecht

Abstract

In Ethiopia both the population and economy are growing rapidly, which results in land cover changes. Over the last decades natural vegetation like forest is replaced by cultivated land and settlements and new cash crops are introduced in parts of Ethiopia. As a result, soil erosion increased in many part of Ethiopia. To assess the effect of land cover change on soil erosion five different land cover and soil conservation scenarios are constructed for a case study in the Tikur Woha catchment. One scenario represents a natural reference scenario, two scenarios represent the increase in cash crops (khat and sugarcane), one scenario is based on current policy that replaces khat on steep slope by forest, and the last scenario represents the current land cover when soil and water conservation is applied. Furthermore, an assessment of the current soil erosion is made. In this study the Soil and Water Assessment Tool is used to quantify the erosion rates of the different scenarios. Better understating of current and possible future erosion rates and their spatial distribution will be of great value in reducing future soil erosion and maintaining food production.

Results show an average soil erosion rate of 4.32 t h^{-1} y^{-1} for the Tikur Woha catchment over the modelled period of 2005-2010 with current land cover. Only 5% of the catchment is exposed to erosion rates above 15 t h^{-1} y^{-1}. The lowest erosion rates are found for the reference scenario with an average soil erosion rate of 0.12 t h^{-1} y^{-1}. When the reference scenario is excluded, the soil conservation scenario results in the lowest average erosion rate (3.26 t h^{-1} y^{-1}), and is the most effective in reducing soil erosion in most the sub basins. The policy scenario is less effective in reducing average soil erosion rates (4.00 t h^{-1} y^{-1}). The two cash crops scenarios show a negative (4.68 t h^{-1} y^{-1}) and a small positive effect (3.46 t h^{-1} y^{-1}) on soil erosion rates. If the current land cover trend continues and both natural land cover and agricultural land cover are replaced, soil erosion rates will increase. Therefore, policy should focus on implementing soil conservation and restoring and maintaining natural vegetation to reduce soil erosion rates in the Tikur Woha catchment.

.

ACKNOWLEDGEMENT

I would like to thank my supervisors Elisabeth Addink and Marjolein Vogels for helping me completing this master thesis. Furthermore, I would like to thank the Wondo Genet College of Forestry and Natural resources for their support during the fieldwork. In particular I would like to thank Kebede Wolka for his help during the fieldwork period in Ethiopia.

CONTENTS

LIST OF FIGURES

LIST OF TABLES

1 INTRODUCTION

Soil erosion is a large environmental problem, especially in developing countries in tropic and sub tropic regions (Lai, 2006). An example of such a country is Ethiopia, one of the least developed countries in the world (Bewket & Teferi., 2009). According to various authors soil erosion is one of the largest environmental problems in Ethiopia (Shiferaw & Holden., 1999, Taddese, 2001, Bewket & Teferi., 2009). Soil erosion can have a large impact on the long term land productivity and can lead to decreasing crop yields over time (Tesfahunegn *et al.*, 2012). Sonneveld (2002) indicated that under a stationary scenario, food production will drop by 30% due to soil erosion by the year 2030, which will result in a strong decrease in food production and food security. Hurni (1989) estimated that most of the top soil of cropland will be eroded within 150 years under the current conditions. Because of the direct dependency of livelihood on agriculture for a large part of the population, the social and economic impacts of soil erosion are large (Tibebe & Bewket, 2010).

Soil erosion is a natural occurring process, but can be enhanced by human influence. In Ethiopia the enhanced soil erosion is mainly caused by land use and land cover changes (Nyssen *et al.*, 2005). The last few decades Ethiopia experienced major land cover changes (Taddesse, 2001). Deforestation, overgrazing, mismanagement of cultivated soils, and expansion of cultivated and residential area are a result of population growth (Blanco-Canqui & Lai., 2008, Tesfahunegn *et al.,* 2012). Currently the population density of Ethiopia is among the highest in Africa, and population growth will continue in the future (Sonneveld, 2002). Beside population growth, economic growth is a driver of land cover change. Changed market conditions and better infrastructure resulted in the introduction of cash crops such as Khat (Dessie & Kinlund, 2008). The high land cover dynamics will continue and will have a large influence on soil erosion rates. To maintain the food production and food security it is of great importance to assess the effect of different land cover and soil conservation on soil erosion rates and the spatial distribution, in order to take effective measurement to reduce soil erosion. In this study the Tikur Woha catchment is used as a case study.

1.1 Erosion Tikur Woha catchment

Because of the severity of soil erosion there are many studies that assess soil erosion in Ethiopia (Hurni, 1989, Hurni & Pimentel., 1993, Tadesse, 2001, Sonneveld, 2002, Nyssen *et al.*, 2004). Although there are numerous studies that assess soil erosion in the northern and eastern parts of Ethiopia only a few studies are done in the Central Ethiopian Rift Valley (CERV). For the CERV, Meshesha *et al.* (2012) conducted the first study that quantified soil loss due water erosion. A soil erosion assessment was made for the period 1973-2006 using the Universal Soil Loss Equation (USLE). They classified Landsat images of the years 1973, 1985 and 2006. Based on the field survey, a 71.1% accuracy of the magnitude of soil erosion was achieved. A strong increase in erosion was observed from the years 1973, 1985 and 2006 with respectively 31, 38 and 56 t h^{-1} y^{-1}. Land cover conversion of forest area to cropland is indicated as the main factor for the increase of soil erosion. Furthermore, they found that if the current land cover trends continue, the already severe erosion will increase with 66% by the year 2020. In the study by Meshesha *et al.* (2012), the Tikur Woha catchment in CERV was excluded. The Tikur Woha catchment is located in one of the most densely populated areas in Ethiopia (Dessi & Kinlund, 2008). While the erosion is mainly human induced, e.g. by land cover change or mismanagement, it is of great importance to estimate the magnitude and spatial extent of soil erosion in a highly populated area like the Tikur Woha catchment.

There is a large uncertainty in the current erosion extent in the Tikur Woha catchment. At present two studies assess soil erosion in the Awassa catchment, which includes the Tikur Woha catchment, and one study assess the soil erosion for the Tikur Woha catchment specifically. The study by MoWR (2010) used the Revised Universal Soil Loss equation (RUSLE) to assess soil erosion rates and Ali & Hagos (2016) used the USLE. The USLE and RUSLE use the same formula for calculating the erosion rates, but the factors are determined in a different way. Both studies show that only a small part of the Awassa catchment experience moderate to severe soil erosion. In the Awassa catchment only 11.2% (MOWR, 2010) and 2.5% (Ali & Hagos 2016) are exposed to erosion rates higher than 11 t h^{-1} y^{-1}. In contrast, Wolka *et al.* (2015) found that more than half (53.6%) of the Tikur Woha catchment experienced severe (45-60 t ha^{-1} yr^{-1}) to extremely severe (80-85 t ha^{-1} yr^{-1}) soil loss due to rainfall erosion. Erosion rates in the catchment were estimated using RUSLE. Most severe soil erosion occurred in the central part of the catchment in Abaro-Wijigira mountain chain, due to topographic factors. Beside the already severe soil erosion in the largest part of the catchment, Wolka *et al.* (2015) indicated that population growth and forest decline will result in higher erosion rates in the future.

Because there is a large variation in the erosion rates for the Tikur Woha catchment, estimations of current erosion rate are needed. Alongside this, it is necessary to investigate the change in erosion rates for possible future scenarios of different land cover and land use management. At the moment, there are no studies that assess the erosion rate in the Tikur Woha catchment under different land cover and land management scenarios.

1.2 Land cover change Tikur Woha catchment

As previously mentioned, land cover is one of the most important aspects that affect soil erosion. In this section, an overview of past research regarding land cover change in and around the Tikur Woha catchment is provided. Muzein (2006) and Meshasha *et al.* (2012) examined land cover changes in the CERV. Wondrade *et al.* (2014) used remote sensing and GIS to map multi-temporal land cover changes in de Awassa catchment. Other studies investigated the effect of land cover changes on hydrology in the Awassa catchment (Wolka *et al.*, 2014). Dessie & Kleman (2007), and Dessie & Kinlund (2008) focused their land cover change study mainly on the decline of forest and the khat expansion in de Awassa and Wondo Genet area.

On a larger scale Muzein (2006) and Meshesha *et al*. (2010) used Landsat thematic mapper (TM) and Landsat Multi-Spectra-Scanner (MSS) satellite images to assess and analyse land cover changes in the CERV. Satellite images for the year 1973 and 1986 were used for both studies, together with the satellite image of 2000 (Muzein, 2006), and 2006 (Meshasha *et al*., 2010). Classification accuracies for both studies range from 82% to 89%. For the classification Muzein (2006) used a supervised maximal likelihood classification, Meshesha *et al.,* (2010) combined a supervised and unsupervised classification method. In both studies the land cover classes forest and woodland showed the strongest decrease. The decrease of forest area range from 64-70% and de woodland area decreased with 55-69%. The forest decline is also observed on a national level (Berry, 2003; Nyssen *et al.*, 2004). Agricultural area showed the largest increase in both studies, although the order of magnitude is different. In the study of Muzein (2006) an increase of 115 % of agricultural area is observed, Meshesha *et al*. (2010) found a smaller increase of agricultural land (45 %). The growth of the population and livestock are indicated as the main driver for the reduction in forest area and the increase in agricultural area.

For the Awassa catchment Wondered *et al.* (2013) assessed the land cover change between 1973 and 2011 using Landsat MSS and Landsat TM satellite images using a combined supervised and unsupervised classification. The satellite images were classified into nine land cover classes with an accuracy between 82.5% and 85%. Dessie & Kleman (2007) used the Landsat MSS and Landsat TM satellite images of the years 1972 and 2000 to identify the forest decline in the area using a supervised maximal likelihood classification. The accuracy of the obtained forest cover maps was 87%. In the period, forest cover decreased 82%, from 16.0% of forest cover in 1972 to 2.8% cover for the year 2000 (Dessie & Kleman, 2007). A large part of the remaining forest is characterised by non-connected patches, because of clearing for farmland and settlements. A smaller forest decline of 54% was found by Wondrade *et al*. (2013). A large increase in built up area is observed by Wondrade *et al.* (2013), built up area increase with 486%, of which the main increase is in the more recent year. Furthermore, agricultural area increased with 29%, because of population growth. Although Dessie & Kleman (2007) did not quantified the increase of urban and agricultural area, they indicated population growth and consequently an increase in settlements, roads and farmland as the main driver for the forest decline. They estimated that smallholder farming accounted for 80 % of the forest loss.

The land cover studies above show a long-term land cover trend of forest decline in combination with an increase of agriculture land and urban area. This land cover trend is both observed on a national scale as well on a regional scale. When land cover changes are assessment on a more regional scale, a more recent land cover trend is observed. Wolka *et al.* (2014) preformed a supervised classification of Landsat images for the years 1986, 1999 and 2011 to analyse land cover changes and the effects of these changes on the water quality and stream flow of rivers to Lake Awassa. As part of the study a land cover assessment was made of the Tikur Woha catchment. Between 1986 and 1999 different land cover trends were observed than in the following period 1999 till 2011. In the first period, there was an increase of cropland of 56.6%, 11.3% decrease of forest, 21.9% decrease of grassland and 28.7% increase of woodland. For the second period, there was an 75.9% decrease of cropland, 49.2% decrease of forest, 79.7% increase of grassland, and 65.5% increase of woodland. The increase of woodland can partly be explained with the introduction of cash crop khat in the 1980’s and the increase of agroforestry. Beside the increase of khat, the amount of sugarcane and enset farming increased in the area in favour of cropland. The decline of food crops (cropland) in favour of khat, sugarcane and enset is also observed by Dessie & Kinlund (2008). The number of farmers that that cultivate khat, sugarcane, and enset increased in the period 1985-2002. In the studies of Dessie & Kinlund (2008) and Wolka *et al.* (2014), a shift from food crops to cash crops since the mid 80's was observed in the Tikur Woha catchment.

1.3 Objectives

The aim of this study is to assess the effect of land cover and soil conservation on soil erosion rates, five different land cover scenarios are constructed for a case study in the Tikur Woha catchment.

The main objective of this study is:

- Estimate the current erosion rates and the effect of land cover and soil conservation on erosion rates of the Tikur Woha catchment.

More specifically:

- Determine current land cover based on high and medium resolution satellite images.
- Determine the magnitude of current erosion rates in the Tikur Woha catchment.
- Estimate the magnitude of erosion for different land cover and soil conservation scenarios.
- Determine optimal allocation of land cover and land management.

2 SITE DESCRIPTION

The Tikur Woha catchment is the focus area of this study and is located in the southern part of CERV, 260 km south of the capital Addis Ababa (Figure 1). The catchment is a sub catchment (670km^2) of the Awassa catchment that drains into Lake Awassa. Nine rivers drain into the Cheleleka wetlands of which the Wosha, Worka, Wedesa and Halo are perennial streams. The Tikur Woha River connects the Cheleleka wetlands and Lake Awassa.

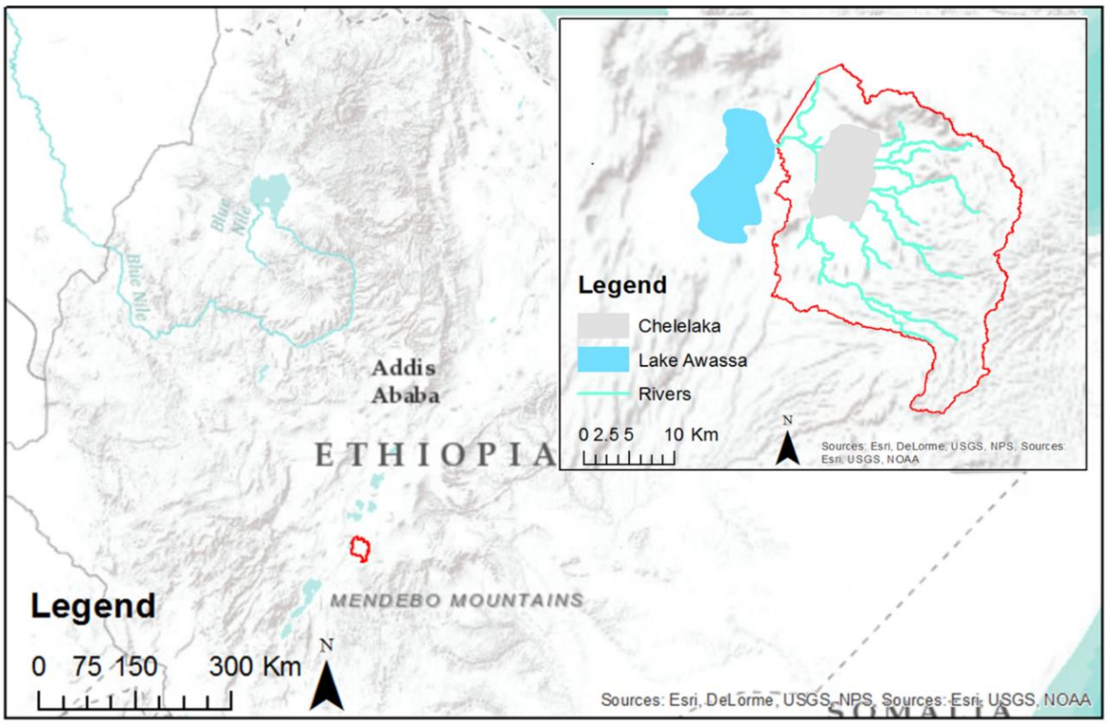

Figure 1: Location of the Tikur Woha catchment, in the right upper corner a detailed map of the of the study area.

2.1 Topography and Soil

The Tikur Woha catchment is located in an old caldera, which has a large influence on the topography. Altitudes in the Tikur Woha catchment range from 1642-3000 meters above sea level (m.a.s.l.) (Figure 2A). The Abaro-Wijigira mountain chain is the border between the lowland in the west and the plateau in the east and southern part of the catchment. The area between the lowlands and the plateau is characterized by steep slopes.

The major soil groups in the study area are Cambisols, Luvisols and Andosols. TCambisols are located in the middle and western part, the Luvisols are mainly located in the south-eastern part, and the Andosols are located in the northern part of the study area (Figure 2B). The Cambisols are moderate to deep soils with a fine to coarse texture, while the Luvisols are very deep soils with a fine to medium texture. Both soil types are highly weathered and are moderately susceptible for erosion. The Andosols are deep to very deep soils with a medium to fine texture. Below a depth of 40 cm the soil is mostly pumic, this soil type is relatively sensitive to soil erosion The Leptosols are shallow to very shallow soils with a coarse texture and is the most sensitive to soil erosion (MoWR, 2010).

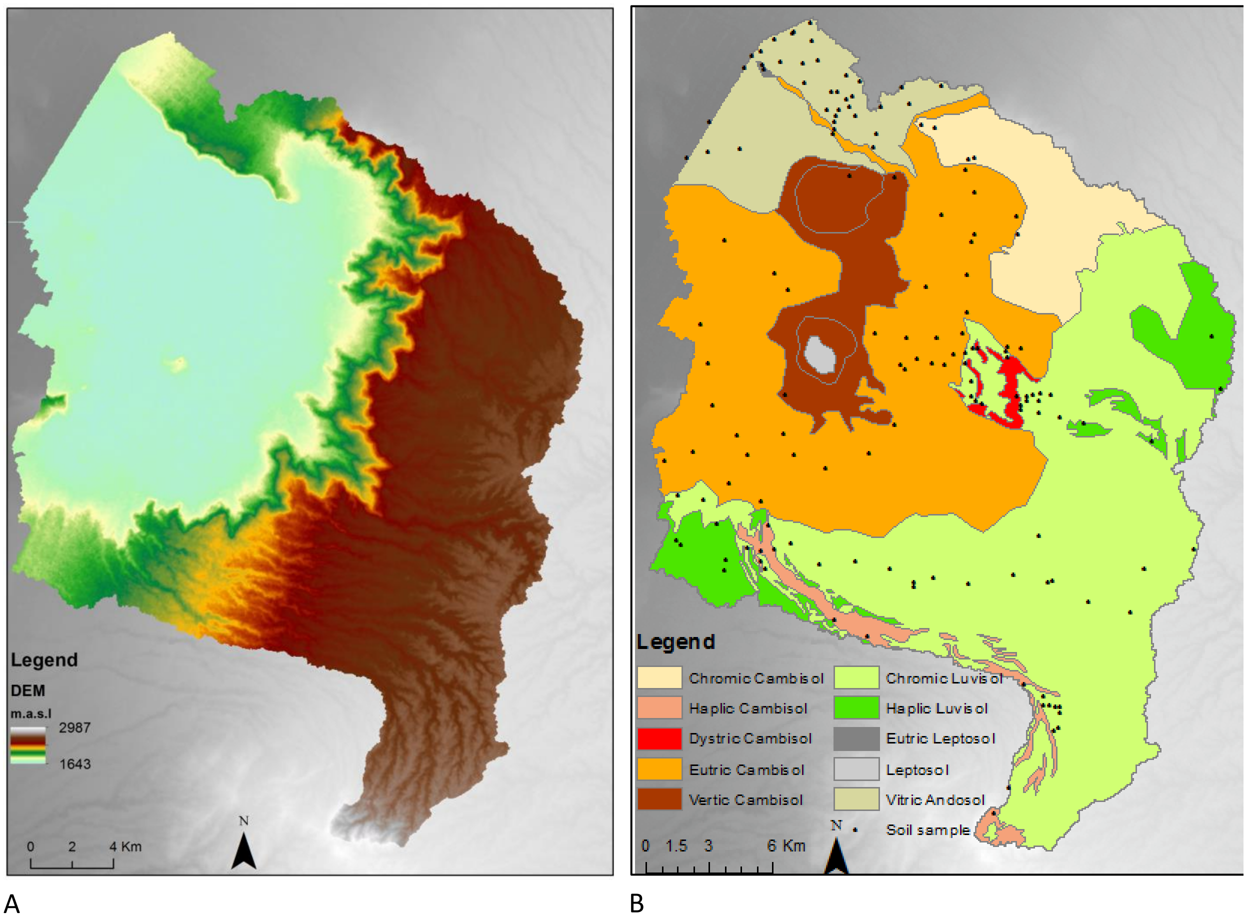

Figure 2: Digital elevation model of the Tikur Woha catchment in m.a.s.l. (A) Soil map and soil sample locations of the Tikur Woha catchment (B) based on the soil map of MoWR (2010).

2.3 Climate

The catchment is characterized by a moist sub-humid to semi-arid climate. The annual amount of rainfall is 1200 mm and the annual temperature is 17°C (Dessie & Kinlund, 2007). The study area is characterized by two rain seasons. The main rain season is between July and September and is responsible for 50-70% of the annual rainfall. The smaller rain season is between February and April and is responsible for 20-30% of the annual rainfall (Legesse *et al.*, 2004). The dry season extends between October and February. The bimodal rain season results in two different crop seasons, with the main crop season occurring between September and February and the second crop season between May and August.

2.4 Land cover

In the study area, land cover is strongly influenced by altitude, soil and, precipitation. The current dominant land use type in the Tikur Woha catchment is small perennial crop farming, with an average plot size of less than half a hectare, mostly with enset, khat and sugarcane. Other agricultural crops include maize, teff, and potatoes (Dessie& Kleman 2008). The western part of the catchment is dominated by commercial farming. Maize and sugarcane are the main crop types in the area and are cultivated on relative large plots. Beside the cultivated land, the main urban areas are located in the western part of the study area. The city Awassa is located next to Lake Awassa; other urban areas are located along the main road that runs in north south direction in the middle of the catchment. East to the city Awassa, the Chelelaka wetland is located. The eastern and southern part of the catchment are characterized by smaller plots. The slopes are cultivated with a perennial crop like enset and khat. The slopes in the north-eastern part of the catchments are covered by natural forest. The plateau in the east the land cover is dominated by a mixture of enset and seasonal crops like maize (MowR, 2010).

3 METHOD

3.1 Input data

3.1.1 Field data

Field data was collected during a fieldwork from September till December 2015 (Figure 3). Ground truth for the classification was collected on field scale. Fields were selected based on land cover, field size, spatial location, altitude, soil type, and accessibility. Land cover types were selected based on literature and field observations. Fields with a radius larger than 10m, covered with a representative land cover were used for minimum field size. Locations for collection ground truth data were chosen in such a way that the different soil classes and altitudes were covered.

GPS points were collected in the field together with sketches and photos of the fields. The field data was used to draw field polygons on the Worldview 1 (Digital Globe Inc.) panchromatic imagery with a resolution 0.5 m of October 2008, available as World imagery base layer in ESRI ArcMap 10.2 (Figure 4A). In total, 219 field observations were made and were then used to create field polygons. The field polygons were divided into 17 different land cover classes (bamboo, banana, bare soil, beans, carrot, coffee, enset, forest, grassland, khat, maize, potatoes, shrub land, sugarcane, teff, tree plantation and wheat). Beside land cover, the following characteristics were collected: condition of the plants, cover percentage, and arrangement of the crops.

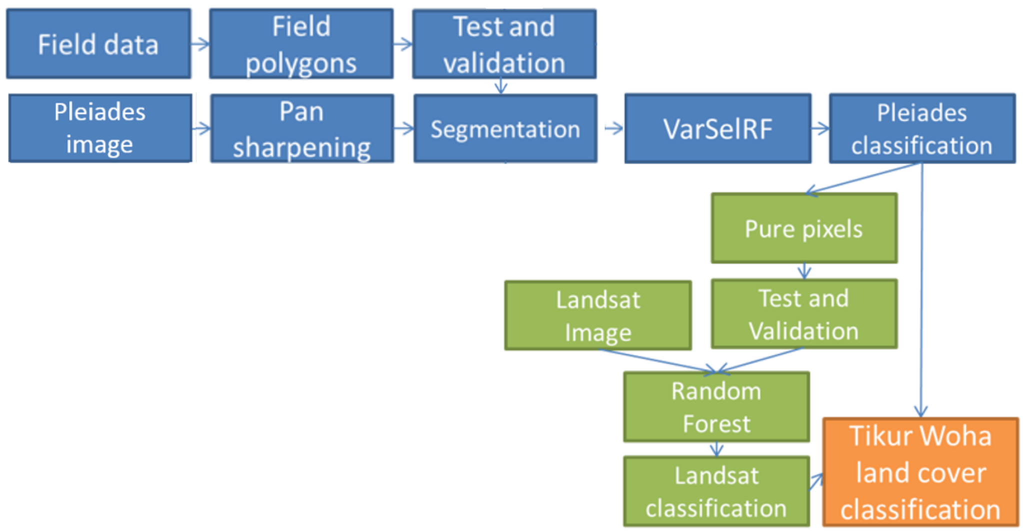

Figure 3: Schematic representation of the land cover classification process of the Tikur Woha. The classification of the Pleiades image is given in blue, the Landsat classification is given in green, and the final product is given in orange. VarselRF= variable selection random forest.

3.1.2 Pleiades Image

The Pleiades A-1 satellite is a high-resolution satellite launched on 16 December 2011. The sensor has five spectral bands, producing a panchromatic and a multispectral image. The panchromatic image (470 – 830nm) has a spatial resolution of 0.5m. The multispectral image has a spatial resolution of 2m and has a blue (430 – 550nm), green (500 – 620nm), red (590 – 710nm) and a near infrared (740 – 940nm) band. For this study, a satellite image was acquired on 17 November 2015 covering an area of 100km^2(Figure 5A).

The panchromatic band and the multispectral bands were used to create a pansharpened image. Pansharpening was applied to make use of both the spectral information of the multispectral band and the more detailed texture information of the panchromatic band. Pansharpening is the process of merging a high resolution panchromatic image and a lower resolution multispectral image to one high resolution multispectral image (Figure 5B, Figure 5C, Figure 5D). Before pansharpening, the panchromatic and multispectral bands were radiometrically corrected. After correction, the Gram-Schmidt pansharpening method was used to create the high resolution multispectral map. The Gram-Schmidt pansharpening is based on the Gram-Schmidt orthogonalization. First, the panchromatic band is transformed to a low-resolution band by computing a weighted average of the multispectral bands. The following weights are assigned to each band 0.9 (red), 0.75 (green), 0.5 (blue), and 0.5 (near infrared) (Laben & Brower, 2000). In the second step, the bands are decorrelated using the Gram-Schmidt orthogonalization algorithm, with each band treated as a multidimensional vector. The low resolution panchromatic band is used as the first vector. After this process, the low resolution panchromatic band is replaced by the high-resolution band and all bands are back transformed into high resolution multispectral bands (Mauer, 2013).

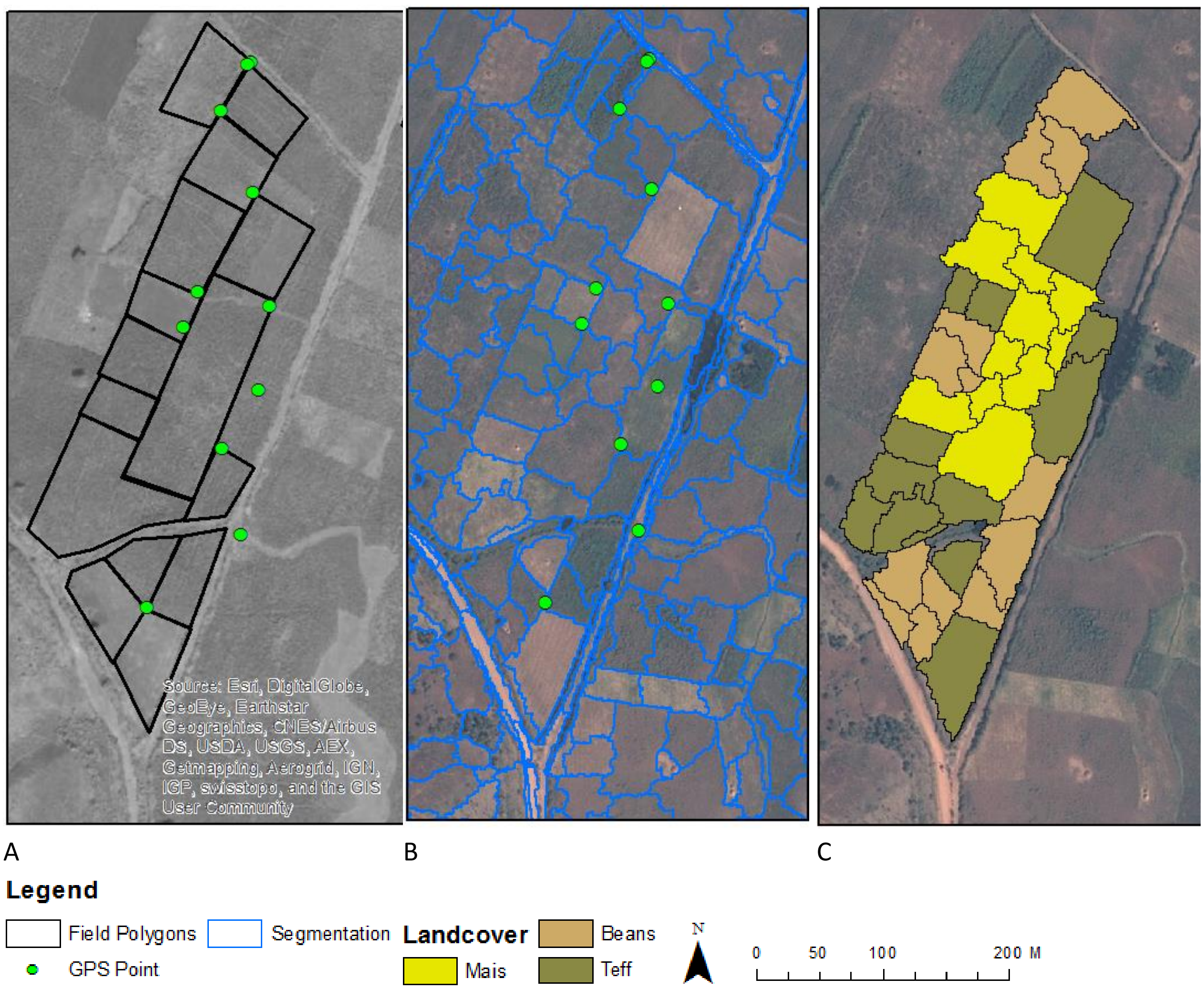

Figure 4: Field polygons and GPS point (A). Segmentation process (B). Classification of segments (C).

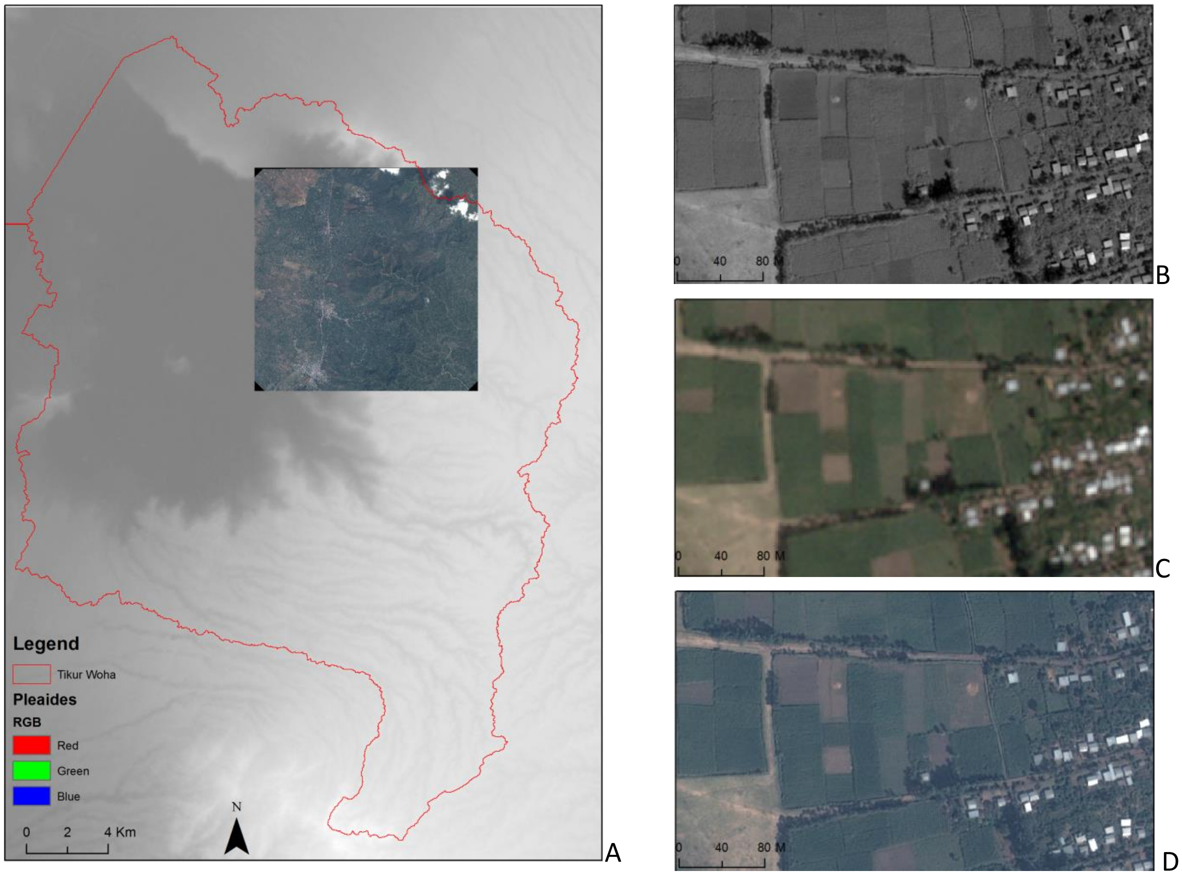

Figure 5: Location and spatial extent of the Pleiades satellite image (A). Detail of the panchromatic Pleiades satellite image (B). Detail of multispectral Pleiades satellite image (C). Detail of pan sharpened Pleiades satellite image (D).

3.1.3 Landsat 8 Image

The Landsat 8 satellite is a medium resolution satellite launched on 11 February 2013. Of the nine bands that are available on the Landsat 8 sensor, seven bands were used for the image classification. The bands that were used are the coastal aerosol (430-450 nm), blue (450 - 515 nm), green (525-600 nm), red (630-680 nm), near infrared (845-885 nm), and two short wavelength infrared (1560-1600 nm (1), and 2100-2300 nm (2)) band, all with a spatial resolution of 30 m. The Landsat 8 image (scene P168, R55) was acquired on 21 November 2015. Before classification, the satellite image was radiometrically corrected.

3.2 Classification process

3.2.1 Object based image and pixel based image analyses

With the higher availability of high resolution satellite imagery, object-based image analyses emerged as an alternative for pixel based image classification. Instead of classifying pixels, groups of pixels (image objects) in an image are classified. An image object is defined as a discrete region of an image that is internally coherent and different from its surrounding (Castilla & Hay, 2008). The advantage of object-based classification is that more information can be used compared to a single pixel. Beside the layer values of each pixel, information like the mean, difference, and standard deviations between pixels in an object can be used. Furthermore, objects have additional spatial information like shape, size, texture and position that can be used to classify an image (Blaschke, 2010).

Beside the object-based classification of the high-resolution Pleiades satellite image that covers a large part of the north eastern part of the catchment, a classification of the whole Tikur Woha catchment is made based on a Landsat 8 satellite image. Because the pixels of the image and objects that needed to be classified are in the same order, for example the size of an agricultural fields and a pixel, a pixel-by-pixel based classification is an appropriate classification technique to apply to the image (Blaschke, 2010). Because classification was based on pixels instead of objects, variables like texture and shape cannot be included in the classification. The classification was only based on spectral value related attributes.

3.2.2 Image segmentation

The Pleiades images is divided into image segments using the multiresolution image segmentation available in the eCognition Developer software (Trimble, 2010). Multiresolution segmentation is region-based algorithm with a bottom-up approach. Individual pixels are merged into larger segments based on their local homogeneity. The homogeneity criterion is combination of spectral homogeneity and shape homogeneity and can be modified by changing the scale parameter. Multiresolution image segmentation allows the distinction between small objects like houses and larger objects like agricultural fields (Baatz & Schäpe, 2000). All four bands of the multispectral Pleiades images were used for the segmentation process, using equal weights for all bands.

For the segmentation process scale, shape and compactness parameters are selected. The scale parameter defines the spatial scale of the segments; larger values result in larger objects. The scale parameter determines the maximum allowed heterogeneity of the image objects. The shape parameter determines the weight of the shape of a segment for the segmentation process, by adjusting the shape value the relationship between the shape and the spectral value changes. When a high shape parameter is chosen, the influence of the spectral value is smaller in the segmentation process. The compactness parameter was the last parameter that was defined. When a higher value is chosen, a more compact object may be made.

Scale, shape and compactness factors are selected by trial and error. The scale factor is selected based on the representation of cultivated fields, without losing smaller objects like buildings. A scale factor of 100 was selected as the appropriate scale factor (Figure 4B). High values are chosen for shape (0.8) and compactness (0.7) parameters, meaning a small influence of spectral values and allowing compact segments. For each segment, 52 different attributes were calculated, of which 27% is shape related, 15% is neighbour related, 31% is texture related, and 27% is related to the layer value of the object. Texture related attributes are based on the grey level co-occurring matrix (GLCM) after Haralick *et al.* (1973). A relatively large number of attributes is selected because a selection of the most important variables will be made. The selection of the attributes was partly based Vogels*, et al.* (unpublished), but the number of attributes was extended because a multispectral image was classified in this study instead of a black and white photo. The number of attributes per class are roughly equally distributed because their importance in the classification process was unknown beforehand.

3.2.3 Test and validation data

The segments and the field polygons that were created using the method described in the previous sections were used to generate a training and validation set (Figure 4C). Segments that fell for at least 75% into the field polygons were classified into one of the 17 land cover classes that were identified during the fieldwork. Five land cover classes (bamboo, banana, carrot, coffee, potatoes and wheat) were deleted for the dataset, because less than 10 segments were classified. Furthermore, the land cover class bare soil was deleted from the dataset. Because of the time lag between ground truth observation and the Pleiades satellite image, fields where bare soil was observed were covered with vegetation on the Pleiades image. When possible, the objects were reclassified into another land cover class (sugarcane and teff) based on fieldwork and the Pleiades images. Otherwise, the objects were deleted from the training and validation dataset. Furthermore, the land cover urban was added to the data set. Segments that represented urban areas were manual selected and classified, based on the Pleiades image. The same method was applied to classify clouds in the image. Both urban land cover class and cloud cover segments were spatially distributed over the study area. Besides removing and adding classes, the land cover class sugarcane and khat were subdivided into small (plant height less than 1 m) and large (plant height above 1 m) categories due to a large difference between small and large sugarcane and khat observed in both spectral and optical profiles (Figure 6). The subdivision is made to reduce confusion between the land cover classes in the classification process. In total, 708 objects were manually classified into 14 different classes. The total dataset was divided into a training and validation dataset. For the training set, 2/3 of the data was used, with the remaining 1/3 used as the validation set.

The classified Pleiades image was used as training and validation set for the Landsat 8 satellite image. Only pure pixels were used as training and validation data. Pure pixels were defined as Landsat pixels that were cover by one land cover class in the Pleiades image. Pure pixels that fell into cloud cover class either on the Pleiades image or the Landsat image were removed from the dataset. New cloud cover pixels for the Landsat images were manually selected and added to the training and validation dataset. Furthermore, an extra land cover class (wetlands) was added to the dataset because this land cover class was absent in the Pleiades image. Areas in the wetland were manual selected based on field knowledge and the Landsat image. The areas were distributed over the wetland to cover the heterogeneity of the wetland.

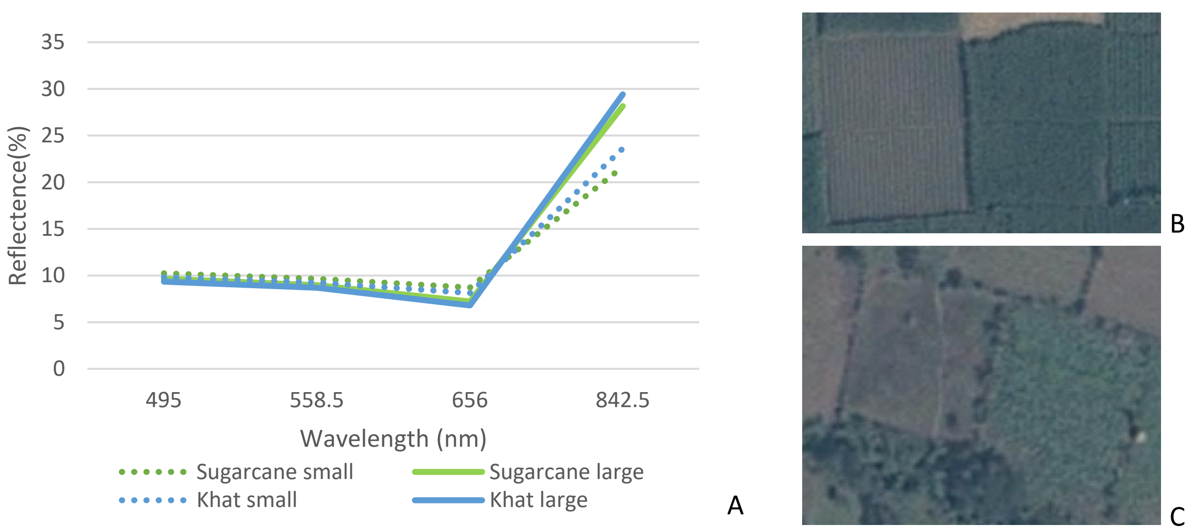

Figure 6: Spectral profiles of sugarcane and khat (A). Optical difference between small sugarcane (left) and large sugarcane (right) (B). Optical difference between small khat (left) and large khat (right) (C).

3.2.4 Random forest

For classification of the objects, the random forest algorithm was used. Random forest is a robust statistical technique which generates multiple decision trees based on a training set in order to make a prediction based on a set of independent variables (Breiman, 2001). The independent variables are used to split the training set into subdivisions until all objects of the training data are classified. In this study, the random forest R-package VarSelRF (Diaz-Uriarte, 2007) was used for the classification. Besides running the random forest algorithm, this package removes the variables that are the least predictive in the classification process. The default settings of the random forest package were used, except for the number of trees which was set on 10,000 to get a more stable result. Trees were built using a 2/3 bootstrap of the training set. The other 1/3 of the training set is used to estimate performance of the random forest, called the Out-Of-Bag (OOB) estimate of error. The OOB error is an indication of how well the classes can be separated (Rodriguez-Galiano *et al.*, 2012).

3.2.5 Classification accuracy

The classification accuracy was assessed by computing a confusion matrix and its derivatives. The overall accuracy is computed by dividing the total number of correct classified objects by the total number of objects in the confusion matrix (Congalton, 1991). Another indicator that is used to assess the accuracy of the classification is the Kappa coefficient. The Kappa coefficient has the advantage over the overall accuracy, because the Kappa coefficient takes chance into account. The Kappa coefficient is calculated based on the difference between actual agreement and the agreement expected by chance (Landis & Koch, 1977).

Beside the overall statistics of the classification, class specific statistics were calculated. Widely used class specific statistics are the producer's accuracy and user's accuracy. These accuracies were calculated in a similar way as the overall accuracy. The producer's accuracy is calculated by dividing the number over correct classified reference objects by the total number of reference objects of that class. It indicates the probability that a reference object is classified correctly. The user's accuracy is calculated by dividing the total number of correctly predicted object by the total number of predicted objects of a specific class. It is an indicator of the probability that a classified object on the map represents land cover on the ground (Congalton, 1991).

3.3 SWAT model

The Soil and Water Assessment Tool (SWAT) was used to model the current erosion rates and the erosion rates for different scenarios for the Tikur Woha catchment. SWAT is a physically based model that was developed to predict the effect of land management practices on water sediment and chemical yield on a catchment scale (Neitsch *et al.*, 2009). In the model, the catchment is divided in sub catchments based on topographic characteristics. The sub catchments are further divided into hydrologic response units (HRUs), which have homogeneous land cover, management and soil characteristics.

The hydrology model in SWAT estimates the surface runoff volume and the peak runoff. This information is used to calculate the runoff erosive energy variable. Surface runoff volume is calculated using a modified version of the curved number method (USDA Soil Conservation Service, 1972). The peak flow calculations are based on the rational method, which means that after a rainfall event runoff will increase until all sub basins contribute to the flow at the outlet. Both the surface runoff and peak runoff are calculated per HRU in SWAT.

The erosion component of the SWAT model is calculated with the Modified Universal Soil Loss Equation (MUSLE) (Equation 2).The MUSLE is based on the USLE (Wischmeier & Smith*,* 1978). While the USLE and the RUSLE predict soil erosion as a function of the rainfall energy, the MUSLE predicts soil erosion based on the runoff factor (Neitsch *et al.*, 2009). Because the MUSLE calculates the erosion based on a runoff factor, no ratio between the rainfall energy and soil erosion has to be used. Furthermore, the runoff factor accounts for more soil erosion variation than the rainfall energy factor.

$$sed = 11.8\left(Q_{surf} \cdot q_{peak} \cdot area_{hru}\right)^{0.58} \cdot K_{USLE} \cdot C_{USLE} \cdot P_{USLE} \cdot SL_{USLE} \cdot CFRG \qquad \textit{Equation 2}$$

where *sed* is the sediment yield on a given day (metric tons), Q_{surf} is the surface runoff volume (mm H_2O/h), q_{peak} is the peak runoff rate (m^3/s), $\cdot area_{hru}$ is the area of the hydrological response unit (HRU)(h), K_{USLE} is the USLE erodibility factor, C_{USLE} is the USLE cover and management factor, P_{USLE} is the USLE support practice factor, SL_{USLE} is the USLE topographic factor and $CFRG$ is the coarse fragment factor.

3.4 Data input

3.4.1 Topography

The Advanced Spaceborne Thermal Emission and Reflection Radiometer (ASTER) Global Digital Elevation Model Version 2 (GDEM V2) was used as DEM input. The DEM has a resolution of 30 meters, but was resampled to a resolution of 5 meter. Resampling to a finer resolution was done to maintain more land cover details in the modelling process. In SWAT, the grid size of the DEM is used as the spatial resolution.

3.4.2 Land cover data

For the SWAT model, a land cover map that covers the total study area is needed. The land cover map is based on a combination of the high resolution Pleiades image and the lower resolution Landsat image, where the Pleiades image had priority over the Landsat image. On both the Pleiades and Landsat 8 satellite image, cloud cover was present. Where possible, the cloud cover was replaced by the land cover classes of the other satellite image. When this was not possible, the cloud cover was replaced by the dominant land cover class in the surrounding area to get a land cover map with total coverage. The whole land cover map was resampled to a resolution of 5 m using the majority criteria. Land cover characteristics were taken from the ArcSWAT2012 and the MapWindowSWAT2012 crop database (available via www.waterbase.org). The land cover classes: grasslands, shrub land, evergreen broadleaved forest and wetlands without trees were taken from the MWSWAT2012 database, while the other land cover classes were taken from the ArcSWAT2012 database. For tree plantations, the characteristics of crop type eucalyptus was selected, eucalyptus is found in the majority of the three plantations. For the enset land cover class, the crop characteristics of banana were chosen. Enset is also known as false banana and has similar plant characteristic as banana except that its fruits are inedible (MoWR, 2010). The plant type khat is not incorporated in both databases, therefore the most similar tree type (e.g. coffee) in the database was used to represent khat in the model. The coffee plant has similar characteristics as khat, such as plant height, temperature range, altitude range and rainfall range. Furthermore, in Ethiopia, coffee is often used as intercropped with khat (Lemessa, 2001).

3.4.3 Soil data

The soil data is based on the soil map of the Rift Valley Master plan (MoWR, 2010). The soil map is based on 400 soil samples taken in the Awassa catchment. The soil map is made on two different spatial scales, on a catchment scale and on a sub catchment scale. The soil map that is constructed on a sub catchment scale is only made for a selected number of sub catchments. In the Tikur Woha catchment, three selected sub catchments are located. Of the 400 soil samples taken to construct the soil map for the whole Awassa catchment, 151 samples are located in the Tikur Woha catchment (Figure 2A). The two water bodies that were indicated on the soil map are replaced with the surrounding soil type (Vertic Cambisol). During the field work no large water bodies were found on the places that were indicated on the map.

Soil characteristics that are used as input for the SWAT model were taken from the Harmonized World Soil Database v 1.2 (Fischer *et al.,* 2008). The soil texture, organic matter, gravel content, salinity, and compaction are used to calculated water availability, saturated hydraulic conductivity and bulk density using the Soil-Plant-Air-Water (SPAW) model (Saxton, 2006).

The K-factor represents the erodibility of the soil and is calculated using the equation proposed by Williams (1995). The K-factor is calculated based on the clay, silt, sand, and organic carbon content (Equation 3).

$$K_{USLE} = f_{cssand} \cdot f_{cl-si} \cdot f_{orgc} \cdot f_{hisand} \qquad \textit{Equation 3}$$

where f_{cssand} is a factor that represents the coarse sand factor (Equation 4), f_{cl-si} represents the silt clay factor (Equation 5), f_{orgc} represents the organic content factor (Equation 6), and f_{hisand} is the factor for an extreme high sand content (Equation 7).

$$f_{cssand} = 0.2 + 0.3 \cdot \exp\,(-0.256 \cdot m_s \cdot \left(1 - \frac{m_{silt}}{100}\right) \qquad \textit{Equation 4}$$

$$f_{cl-si} = \left(\frac{m_{silt}}{m_c + m_{silt}}\right)^{0.3} \qquad \textit{Equation 5}$$

$$f_{orgc} = \left(1 - 0.25 \cdot \frac{orgC}{orgC + \exp(3.72 - 2.95 \cdot orgC)}\right) \qquad \textit{Equation 6}$$

$$f_{hisand} = (1 - 0.71 \cdot \frac{\frac{m_s}{100}}{(1 - \frac{m_s}{100}) + \exp(-5.5 + 22.9 \cdot \left(1 - \frac{m_s}{100}\right)} \qquad \textit{Equation 7}$$

where m_s is the percentage sand content (0.05-2 mm diameter), m_{silt} is the percentage silt content (0.002-0.05 mm diameter, m_c is the percentage clay content (<0.002 mm diameter), and orgC is the percentage organic carbon of the layer.

3.4.4 Climatological data

Climatological data of the National Meteorology Agency of Ethiopia is used in this study. Weather stations located in or near the study area with the least temperature and precipitation data were selected, which are the weather stations of Awassa, Koffele, and Watereresa. Because of the large amount of missing data only a record of 5 years is used. The precipitation and temperature data for the period 2005-2010 of the weathers stations Awassa, Koffele and Watereresa is as data input. This period was selected because of the low percentage of missing data (<5% for each station). Furthermore, this period was characterised by relative wet year (2006) and one relative dry year (2009). In 2006, there was 26% more precipitation, and in 2009 there was 25% less rainfall than the average rainfall over the period 2005-2010. Besides temperature and precipitation, the SWAT model needs wind, solar radiation and relative humidity as input. This data was obtained from the Texas A&M University spatial sciences website, globalweather.tamu.edu (Globalweather, 2012). Weather simulation of the following coordinates were used 7.065, 38.4870 (Awassa), 7.0251, 38.784 (Koffele), and 6.9181, 38.6854 (Watereresa).

3.4.5 Calibration

The SWAT model is intended for application in ungauged watersheds and therefore the model can be used without calibration (Neitsch *et al.* 2002). However, the SWAT model is often calibrated to improve model outcomes (Mosbahi *et al.*,2013). In this study, the SWAT model was calibrated using river discharge data provided by the National Meteorology Agency of Ethiopia. In total, six parameters were adjusted before running the SWAT model. A relative change of -7.8% and -57.8% were applied to the parameters of the curved number and the available soil water content respectively. New parameter values were assigned to ground water delay (104.5), base flow alpha factor (0.09), soil evaporation compensation factor (0.9), and for the threshold depth of shallow aquifers (659.0). For details about the calibration process see van Dijk (unpublished).

3.5 Scenarios

For this study five different scenarios were made to estimate erosion in the Tikur Woha catchment (Figure 7, Table 1). Besides the five scenarios, current erosion rates were estimated. Because there are uncertainties in both erosion modelling and future land cover, the extremes of the scenarios were taken to get an insight in the order of magnitude of future soil erosion rates. Four land cover scenarios and one soil conservation scenarios were used in this study. One land cover scenario represents a natural reference situation, two scenarios are related to the increase in cash crops and one land cover scenario is based on current policy. The fifth scenario is based on the application of soil and water conservation measurements. The scenarios are based on literature, interviews conducted in the field and field data, a more detailed description is given below.

Table 1: percentages per land cover class for the current land cover and for different scenarios

LAND COVER	CURRENT	REFERENCE	POLICY	CASHCROPA	CASHCROPB
GRASS	4.8%	0.0%	4.8%	0.7%	4.8%
TREE PLANTATION	8.6%	0.0%	8.6%	0.2%	8.6%
MAIZE	15.4%	0.0%	15.4%	0.1%	0.1%
ENSET	20.2%	0.0%	20.2%	9.8%	9.8%
BEANS	3.9%	0.0%	3.9%	0.2%	0.2%
TEFF	0.2%	0.0%	0.2%	0.0%	0.0%
FOREST	4.3%	47.3%	16.8%	1.0%	4.3%
URBAN	3.2%	0.0%	3.2%	3.2%	3.2%
SUGARCANE	8.7%	0.0%	8.7%	32.4%	22.9%
KHAT	25.0%	0.0%	12.5%	52.2%	41.9%
SHRUBS LAND	1.8%	28.4%	1.8%	0.2%	0.2%
WETLANDS	4.0%	24.2%	4.0%	0.0%	4.0%

3.5.1 Reference scenario

In the reference scenario, the current land cover was replaced by vegetation that could be expected in a simplified natural situation. The natural vegetation is based on field observations of natural vegetation and literature. For this scenario, only three land cover classes are used, namely wetlands, broadleaf evergreen forest and shrub land. The location of the wetland is based on the elevation of Lake Awassa and the spatial extent of the current wetland. The low lying areas with an altitude below 1700 m.a.s.l. is classified as wetland. The area between 1700 and 2500 m.a.s.l is classified as forest. All land covers above 2500 m.a.s.l altitude is classified to shrub land. The altitude that divides forest and shrub land is based on natural forest records of Dessie & Kleman (2007) and field observations of natural forest vegetation located in the northern part of the Pleiades image.

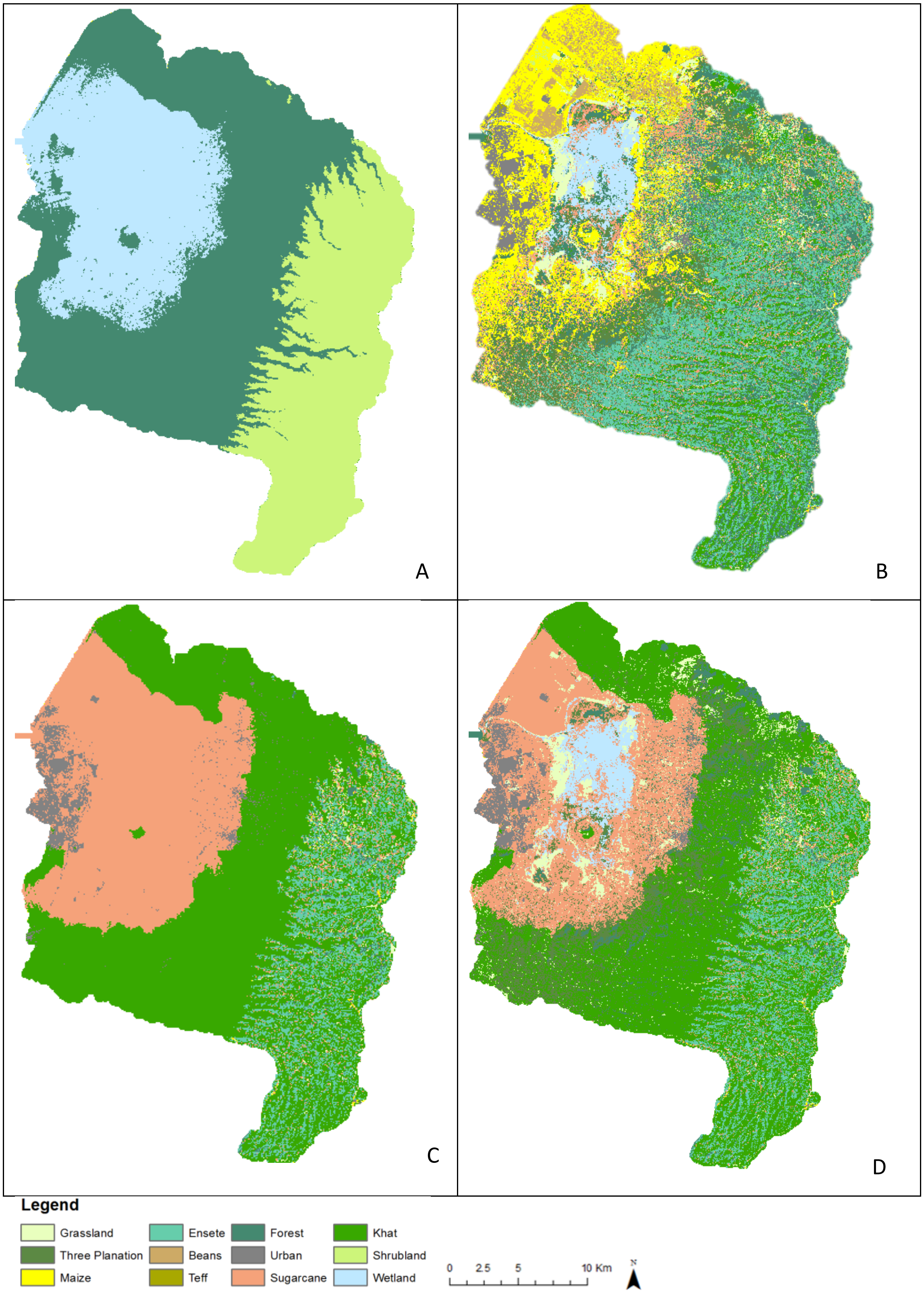

Figure 7: Spatial distribution of land over type of different scenarios, reference scenario (A), policy scenario (B), cash crop expansion A scenario (C), cash crop expansion B scenario (D).

3.5.2 Cash crop expansion scenarios

Various authors (Dessie & Kinlund,2008; MoWR, 2010; Wolka *et al.*,2014) indicate an increase in cash crops such as khat and sugarcane in favor of other agricultural crops and forest in the Tikur Woha catchment. In the cash crop scenario, the effect of the increase of cash crop on erosion rates is estimated. The importance of including the cash crop expansion scenarios in this study is the different effects on soil erosion rates that are indicated by the authors. Dessie & Kinlund (2008) indicated a negative effect on erosion by khat expansion. Because the high value of khat, uncultivated areas such as steeps slopes that are prone to soil erosion, become suitable for khat cultivation. Furthermore, the increase of khat cultivation in these areas results in an increase in permanent settlements near forest areas, which over time can result in more fragmentation and decline of the forest area. Local farmers indicated that khat cultivation has a negative effect on soil erosion (Dessie & Kinlund, 2008). In contrast Wolka *et al.* (2015) indicates a positive effect of more protective land cover types like khat compared to annual cropping systems. Annual crops have a longer period of bare ground in the off-season, which result in more soil erosion due the stronger impact of rainfall and runoff.

Two different cash crop scenarios are incorporated in this study. In both cash crop scenario, the effect of the expansion of the two most valuable crop (sugarcane and khat) per hectare (Dessie & Kinlund, 2008) was modeled. In this scenario, the spatial distribution of the crop type is determined by altitude. The optimal altitude for growing khat in Ethiopia is between 1500- 2500 m.a.s.l (Lemessa, 2001). The optimal altitude for sugarcane range from sea level to 1600 m.a.s.l.. In the cash crop scenario, the altitude divide between the two cash crops is 1750 m.a.s.l. and is based on the current extent of sugarcane in the area. The current extent of sugarcane is used instead of the extent of the optimal growing altitude range because the whole study area is located above 1600 m.a.s.l, and would therefore result in no sugarcane.

The two cash crop scenario differs from each other in type of land cover that is converted into a cash crop. In cash crop scenario A, all land cover up to 2500 m.a.s.l., except for urban areas, is converted to a cash crop. In cash crop scenario B only the agricultural land is converted to a cash crop. Cash crop A is based on the land cover change observed by Dessie & Kinlund (2008) and cash crop scenario B is based on the land cover trend observed by Wolka *et al.* (2014).

3.5.3 Policy scenario

As indicated by Dessie & Kinlund (2008), land that was previously unsuitable for cultivation is converted into khat farms. A large part of the converted land is forest area on steeper slopes. The khat expansion resulted in an increase in illegal forest settlement. As a result, the government took measures to reduce the illegal settlement. During field interviews, it was indicated that large areas with illegal khat farms were cleared by the government. In the khat replacement scenarios, this process of removing khat farms from steep slopes is used. Furthermore, it is assumed that natural vegetation (e.g. forest) will replace the khat farms. In this scenario, all khat areas on steep slopes (>15%) is converted to forest.

3.5.4 Soil conservation measure scenario

Soil and water conservations (SWC) measures on a large scale were introduced in Ethiopia in the 1970s, especially in the northern part of Ethiopia (Wolka, 2014). A strong focus was on the implementation of physical structures. These structures are labour intensive, both to build and to maintain. Furthermore, the physical SWC structures decrease the total area of cultivable land, which has strong implication for farmers, especially in an area like the Tikur Woha catchment where small scale farming is dominant (Dessi & Kleman, 2007). The factors mentioned above resulted in a poor implementation and maintenance of SWC measures in the last 40 years in Ethiopia (Wolka, 2014).

As alternative to structural SWC measures, management practice can have a large influence on soil erosion rates. Contour tillage is indicated by Neitsch *et al.* (2009) as one of the major land use conservation practices, beside terraces and contour striping. Nyssen *et al.* (2000) estimated that tillage erosion contributes half to the total amount of sediment behind stone bunds, which indicates that tillage practice has a strong influence of soil erosion. Temesgen *et al.* (2012) and Muche & Tamesgen (2013) indicate a strong decrease in soil erosion for conservation tillage, like contour tillage, compared to traditional cross ploughing. Temesgen *et al.* (2012) found that conservation tillage could reduce soil erosion between 10% and 51 % for respectively teff and wheat in northern Ethiopia. Furthermore, Temesgen *et al.* (2012) found that farmers were positive towards conservation ploughing and were willing to continue with conservation tillage practice in the future. Because of the relative easy implementation of contour tillage, the positive effect on soil erosion and the positive attitude towards contour tillage of farmers, this conservation will be tested in the soil and water conservation scenario.

In this scenario, the study area without any SWC measures is compared to a situation where contour tillage is fully implemented on cultivated land. The support practice factor that will be used will be based on the values proposed b Wichmeier & Smith (1978). In this scenario, the P-factor will be 0.55 for slopes between 0-15%, 0.75 for slopes between 15-30% and 0.9 for slopes larger than 30%.

4 RESULTS

4.1 Land cover classification

4.1.1 Pleiades

The multiresolution segmentation applied to the Pleiades results in 145426 segments, each with 52 object attributes. Fourteen attributes were selected as most predictive variables by the variable selection. The selected variables are only layer value and texture related attributes; no shape or neighbour relation related variables were selected. The layer value related variables were the spectral values of each band, the maximal difference brightness, Normalized Difference Vegetation Index (NDVI), standard deviation of the red band, and brightness. The texture based variable were the GLCM standard deviation, GLCM mean, GLCM contrast of infrared, GLCM homogeneity of infrared, GLCM dissimilarity of infrared, and the mean of infrared. The selected fourteen variables are used to build the random forest. To assess the accuracy of the random forest the predicted land cover classes are compared to the validation set. A confusion matrix is made to evaluate the difference between the predicted and the reference dataset (Appendix 2A). Besides the confusion matrix, the overall accuracy and the Kappa coefficient and class specific accuracies were calculated to evaluate the classification.

Classification is performed both with and without the subdivision of sugarcane and khat based on height (Table 2). The accuracies of sugarcane are in all cases higher than for khat. For both small sugarcane and small khat, the accuracies are lower than the large class equivalent. Small sugarcane is mainly confused with land cover classes with a relative large part of bare soil like maize, beans, grass, and shrub land. Khat is mostly confused with sugarcane and enset. Classification accuracies are higher when the classification is performed with a subdivision of sugarcane and khat. With the subdivision, sugarcane is less misclassified and khat is better classified, resulting in an overall better classification.

The accuracy assessment was performed with merged sugarcane and khat classes, because this resulted in the highest overall accuracy and Kappa coefficient. The land cover classes were merged after the classification because no distinction will be made between small and large khat and sugarcane in future processing. An overall accuracy of 0.75 and a Kappa coefficient of 0.74 were achieved for the classification.

Beside overall accuracy and Kappa coefficient, class statistic in the form of producer's accuracy and user's accuracy are calculated. Producer's accuracy values range for 0.5 – 1.0 with a mean of 0.74 and user's accuracy values range from 0.38-1.0 with a mean of 0.77 (Appendix 2A). Lowest producer's accuracies are found for enset, beans and khat. The lowest user's accuracies are found for the land cover class enset.

Table 2: Classification with a subdivision gives slightly higher accuracy in all classes.

	Classification based on subdivision of sugarcane and khat						**Classification without subdivision**	
	Accuracy assessment based on separate classes				*Accuracy assessment based on merged classes*			
Land cover	Sugarcane small	Sugarcane large	Khat small	Khat large	Sugarcane	Khat	Sugarcane	Khat
Producer's accuracy	0.54	0.91	0.14	0.65	0.80	0.57	0.74	0.57
User's accuracy	0.56	0.71	1	0.68	0.68	0.74	0.68	0.68
Overall Accuracy	0.75				0.75		0.73	
Kappa Coefficient	0.72				0.74		0.69	

4.1.2 Landsat 8

The Landsat 8 image was classified using the classified Pleiades images. The training and validation dataset had an overall accuracy of 0.75, the overall accuracy of the classification was 0.91. A Kappa coefficient of 0.88 was achieved for the classification of the Landsat image. Producer's accuracy values range for 0.25 – 1.0 with a mean of 0.91 and user's accuracy values range from 0.76-1.0 with a mean of 0.84 (Appendix 2B). Low producer's accuracies were found for the land cover class teff (0.25) and beans (0.65). User's accuracies are higher with 0.76 as the lowest value for the land cover class beans.

4.1.3 Land cover current situation

The current situation was based on the land cover classification of both the satellite images. The high resolution Pleiades land cover classification and the medium resolution Landsat cover classification were combined to create a land cover map for the Tikur Woha catchment (Figure 8, Appendix 1A-1C). The majority of the land cover is cultivated area, of which khat and enset are the main crop types. In the western part of the catchment, maize is the dominant cultivated crop type. The percentage of the different land cover classes is the same for the Pleiades image extent and the whole study area, except for the land cover classes maize, forest and wetland. In both the satellite images cloud cover is low with 1%.

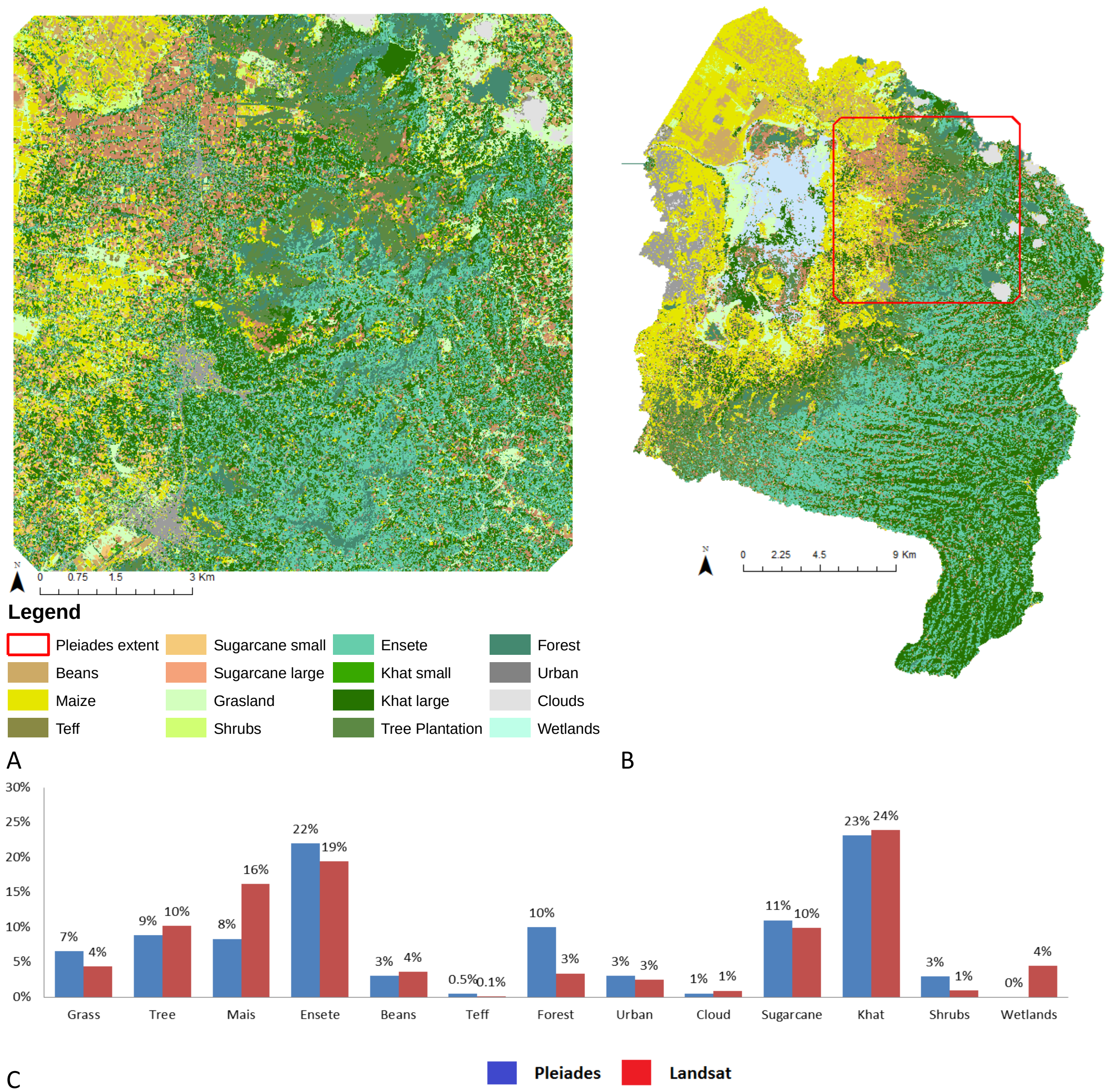

Figure 8: Spatial distribution of land cover of the Pleiades (A) and Landsat (C), together with the corresponding percentage of land cover(C). Detailed maps see appendix 1A and 1B, and 1C.

4.3 Soil Erosion

4.3.1 Current situation

The average soil erosion over the simulated period is 4.32 t h^{-1} y^{-1}, with a maximum of 63.6 t h^{-1} y^{-1} (Figure 9). The average soil erosion for the relative wet year 2006 was 6.84 t h^{-1} y^{-1} and for the relative dry year

2009 the average value was 0.8 t h^{-1} y^{-1} (Figure 10). In the northern part of the catchment, relative high erosion values can be found. The highest erosion rates are associated with the land cover maize, beans, and sugarcane, with an average soil erosion of 12.3, 10.74, and 8.57 t h^{-1} y^{-1}, respectively. The lowest erosion values are related to the land cover classes shrubs, wetland, forest, and tree plantations (Table 3). The highest average erosion rates are associated with the soil classes Vertic Andosols (12.4 t h^{-1} y^{-1}) and Leptosol (10.1 t h^{-1} y^{-1}). For the other soil classes, soil erosion rates vary between 2.9 t h^{-1} y^{-1} and 5.1 t h^{-1} y^{-1}.

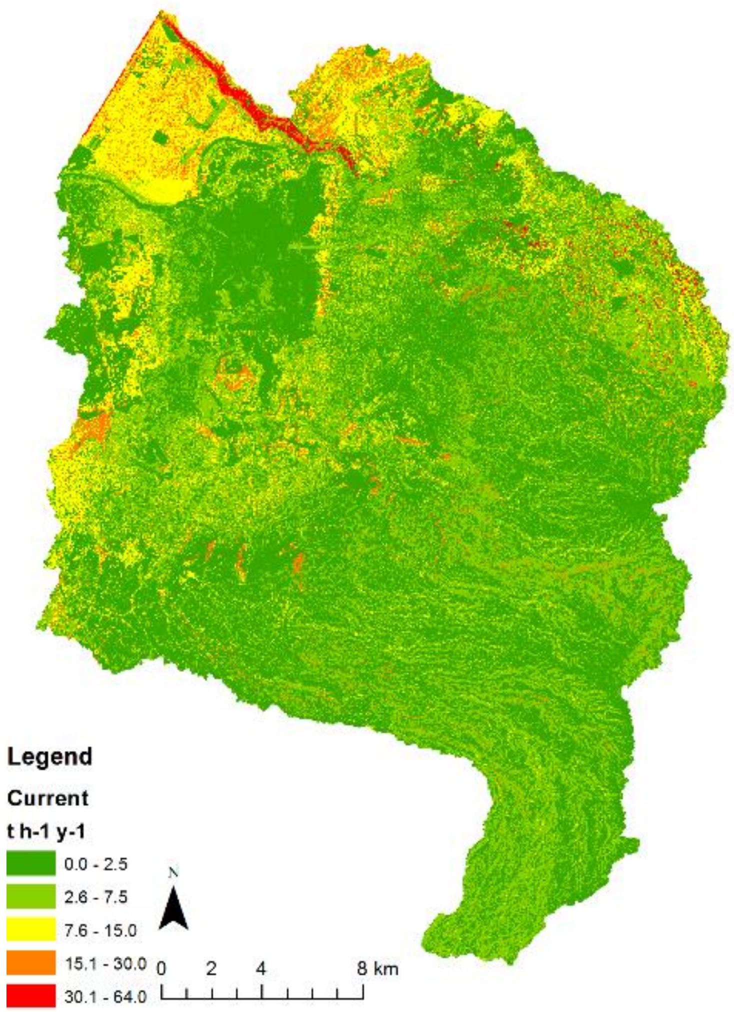

Figure 9: Spatial distribution of average erosion for the period 2005-2010 with current land use

Table 3: Average and maximum soil erosion for the current situation for the period 2005-2010 per land cover class and slope class.

Land cover	Soil erosion		Slope class		
	Average	Max	**0-15**	**15-30**	**>30**
Maize	12.34	46.61	7.89	13.63	25.63
Beans	10.74	26.66	8.35	12.21	16.70
Sugarcane	8.57	63.56	4.50	8.14	18.22
Khat	3.35	14.32	1.83	2.99	5.72
Grassland	2.61	27.06	1.67	2.73	4.97
Ensete	2.19	16.61	0.98	1.65	3.58
Teff	1.25	8.87	0.88	1.42	2.29
Urban	0.65	4.31	0.41	0.73	1.59
Scrubs	0.55	3.67	0.28	0.42	1.14
Wetlands	0.16	9.77	0.13	0.20	0.28
Forest	0.04	1.16	0.02	0.02	0.07
Tree Plantation	0.04	0.20	0.02	0.04	0.06

4.3.2 Scenarios

The spatial distribution of erosion of the five different scenarios, together with the current erosion rates is given in Appendix 3A-3E. The average soil erosion over the simulated period ranges from 0.12 t h^{-1} y^{-1} in the reference scenario to 4.68 t h^{-1} y^{-1} in the cash crop A scenario (Figure 10). In a relative wet year, the highest erosion rates occur with the current land cover, the average soil erosion rate is 6.84 t h^{-1} y^{-1}. In the relative dry year, the lowest erosion rates are found in the reference scenario with an average soil erosion rate of 0.03 t h^{-1} y^{-1}.

In the current situation and policy scenario, the highest percentage of erosion rates above 15 t h^{-1} y^{-1} can be found (Figure 11). Both the cash crop scenarios have a relatively large amount of erosion between 2.5-7.5 t h^{-1} y^{-1} of erosion. Almost all erosion in the reference scenario falls in the lowest erosion category (0-2.5 t h^{-1} y^{-1}).

The spatial distribution of erosion for the policy and SWC shows a similar pattern as the current situation, although erosion rates are lower in some areas. In the two cash crop scenarios, the erosion rates are more equal distributed over the study area. Highest erosion rates are found in the north eastern part of the study area. In the reference scenario, only a small area located in the wetland area experience erosion rates higher than 2.5 t h^{-1} y^{-1}.

When erosion rates of the different scenarios are compared on the sub basin scale, the lowest erosion rates are found in 57 of the sub basins with SWC measure, 16 sub basins with cash crop scenario B, 3 sub basins with the policy scenario, 1 sub basin with both cash crop A and B, when the reference scenario is not taken into account. The cash crops scenarios result in the lowest erosion rates in the northern and western part of the study area. The policy scenario results in the lowest erosion rates in south eastern part of the study area. The average soil erosion rate in this situation is 2.32 t h^{-1} y^{-1}.

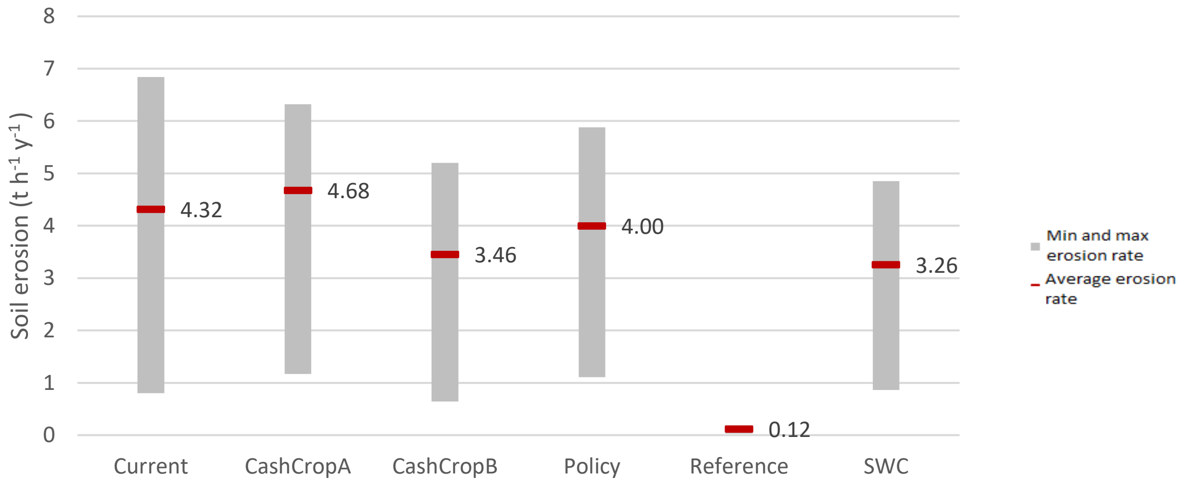

Figure 10:Average soil erosion per year for over the period 2005-2010, together with the erosion rates of the relative dry year 2009 and relative wet year 2006

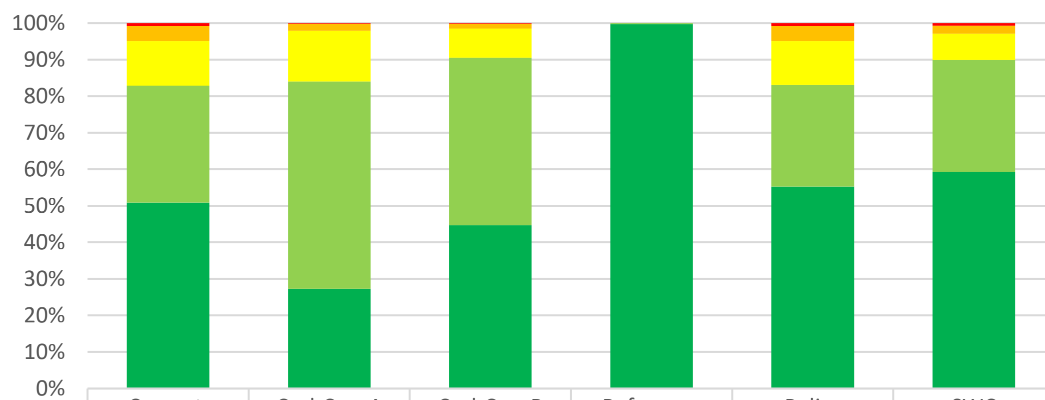

	Current	CashCropA	CashCropB	Reference	Policy	SWC
>30	0.8%	0.2%	0.2%	0.0%	0.8%	0.7%
15-30	4.1%	1.9%	1.3%	0.0%	4.1%	2.2%
7.5-15	12.3%	13.9%	8.0%	0.0%	12.0%	7.2%
2.5-7.5	31.9%	56.7%	45.9%	0.3%	27.8%	30.6%
0-2.5	50.9%	27.3%	44.6%	99.7%	55.3%	59.3%

Figure 11: Percentage of each erosion class of the total study area per scenario. Values are average erosion rates for the period 2005-2010

5 DISCUSSION

5.1 Land cover classification

Overall accuracy values range from 0.75 for the Pleiades image to 0.91 for the Landsat classification. In the literature, different values are used to indicate a good classification result. A strict classification threshold of 0.85 (Anderson, 1976) is widely used to represent a good classification. The classification of the Pleiades does not meet this strict threshold, but an overall accuracy of 0.75 can still be classified as reasonable. Although the overall accuracy of the Landsat classification does meet the threshold, the value is not a reliable indicator for the accuracy because the land cover classes are not equally distributed. When class sizes differ the Kappa value is a better indicator for the accuracy of the classification, because the Kappa statistic corrects for unequal class sizes. There is no universal Kappa coefficient that indicates that a classification is acceptable (Bakeman *et al.,* 2010), but there are multiple guidelines of Kappa coefficients that indicate the accuracy of the classification. Kappa coefficients above 0.61 are indicated as substantial and above 0.80 indicate a good classification (Landis *et al.*, 1977). The Kappa coefficient of the Pleiades classification is 0.74 and for the Landsat classification is 0.88, which indicate a substantial to good classification. The high Kappa coefficient and the higher class accuracy of Landsat compared to the Pleiades can be explained by multiple reasons. First, a larger training and validation was used to build the random forest. Secondly, only pure pixels were used in both the validation and test dataset, which is likely to reduce the confusion between land cover classes. In the classification of the Pleiades images, multispectral information is more important than texture based variables, which is in line with similar studies (Salas *et al.*, 2016).

Relative low producer's and user's accuracy of the classification are found with the land cover enset, especially in the Pleiades image. This land cover class is often confused with khat and tree plantation. Similarities in spectral profiles and texture, because of the crop arrangement in lines, can be an explanation for the confusion. Furthermore, khat and enset are often located near each other, and are sometimes intercropped, which can lead to misclassification. The relatively large confusion between maize and beans can be explained by the long-time lag between ground truth observations and the date of the satellite image. During the field period, it was observed that some maize fields were harvested and replanted with beans.

The spatial distribution of land cover is in line with field observations and the land cover distribution given by MoWR (2010). The land cover class forest is likely to be over predicted in the classification. The forest cover of 10 % in the Pleiades extent is much higher than the forest covers of 2.8% indicated by Dessie & Kinlund (2008) for roughly the same area. The first reason for the over predication of forest area are cloud shadows. No correction was applied for cloud shadows; these darker areas are often classified as forest. The second reason for an over prediction of forest area is that no topographic correction was applied to the satellite images. Because the satellite image was taken in the morning, the low sun angle created shadows on some of the slopes. These dark areas are often classified as forest area. The difference in forest area in the Pleiades image and Landsat image can be explained by the spatial distribution of forest in the area. A relative large natural forest is located in the northern part of the catchment. The difference is likely not related to cloud shadows because the same amount of cloud cover was observed in both images.

The three biggest land cover classes are khat, enset, and maize in both the Pleiades and Tikur Woha classification. This is in line with the dominant cultivated land cover classes indicated by MoWR (2010), with maize mainly located in the western part of the Awassa catchment. Although the major land cover classes are in line with MoWR (2010), there is an over predication of khat and enset in the south-eastern part of the study area. The over predication is partly due shadows created by the topography. Another reason for the over predication in this area is the location of the test and validation data. A large part of the test and validation data is located in lower and drier area, compared to the plateau which is higher and wetter. Due to accessibility constrains the plateau area was less accessible during the fieldwork. The difference in local conditions resulted in difference between spectral profiles of the same plant type in different locations. The spectral profile of grassland on the plateau is more in line with the spectral profile of khat than the spectral profile of grassland in the lowlands where most of the ground truth data is collected (Figure 12). Therefore, grassland on the plateau is sometimes misclassified as khat.

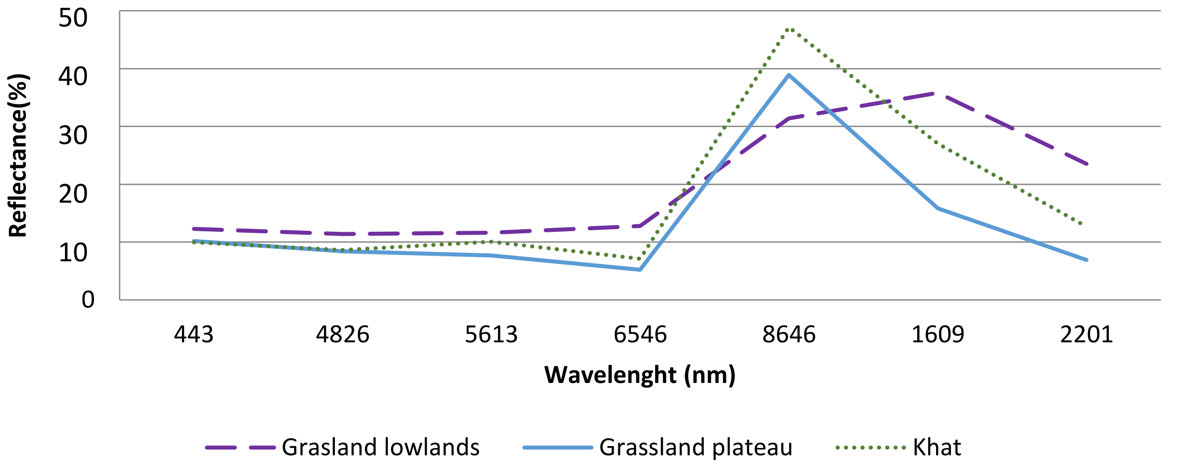

Figure 12: Spectral profile on grassland in the lowlands, grassland on the plateau and khat.

5.2 SWAT Model

The SWAT model is intended for application in ungauged watersheds and therefore the model can be used without calibration (Neitsch *et al.* 2002). However, the SWAT model is often calibrated to improve model outcomes (Mosbahi *et al.*,2013). In this study, only a simple calibration based on river discharge is applied. This was done because the main aim of this study is to assess the effect of different land cover on soil erosion rates and the spatial distribution rather than estimating the exact erosion rates. However, the model could improve when further calibration is done, especially when the model is calibrated on soil erosion rates rather than river discharge.

In this study, land cover characteristics of the ArcSwat2012 and WMSWAT2012 are used. Most land cover classes were available in these databases except from enset and khat. In this study the most similar land cover types are used e.g. banana and coffee. Although the used crops are comparable to enset and khat, the model could improve by including these land cover classes. Especially because khat and enset are large land cover classes and play an important role in the land cover scenarios. Furthermore, as indicated by Griensven *et al.* (2012), better results can be obtained by adjusting the crop parameters local conditions, however this is beyond the scope of this study.

5.3 Erosion current situation

As described in the introduction, there is a large uncertainty in the magnitude of the current erosion in the study area. Wolke *et al.* (2015) showed that more than half of the Tikur Woha catchment experience severe soil erosion (>45 t h^{-1} y^{-1}). On the other hand, two studies that estimated soil erosion for the whole Awassa catchment show that the majority of the catchment is not exposed to severe soil erosion. In the study by MoWR (2010) 88.8% of the catchment has less than 11 t h^{-1} y^{-1} of erosion. A recent study of Ali & Hagos (2016) showed that 97.5% of the Awassa catchment experienced less than 10 t h^{-1} y^{-1}. This study shows that 82.8% of the Tikur Woha catchment experience less soil erosion than 7.5 t h^{-1} y^{-1} with the current land cover, and is therefore more in line with both studies of the Awassa catchment. The average soil erosion of the Tikur Woha fall in the range of 'tolerable' soil erosion rates of 2-18 t h^{-1} y^{-1}(Hurni, 1995). In the study area only a small part of 5% is exposed to non-tolerable erosion rates. Higher erosion rates are mainly found in areas where agricultural land is located on steeper slopes. Maize, beans and sugarcane on slopes steeper than 30% all show average soil erosion rates above 15 t h^{-1} y^{-1}.

Beside comparing the soil erosion rates with studies in the same area, a comparison is made with a soil erosion study in a different area with similar conditions by Tebebe *et al.* (2010). They estimated soil erosion rates using the SWAT model in the Keleta watershed, located north of the Tikur Woha catchment. The watershed is 1060 km^2 and has comparable watershed characteristic. In the studies, the SWAT model was calibrated using surface runoff. Although the SWAT model of the study by Tebebe *et al.* (2010) is more extensively calibrated than the model in this study, very similar erosion rates are found. On average, the soil loss was 4.26 t h^{-1} y^{-1}, the maximum erosion over the modelled period 1980-2000 was 7.57 t h^{-1} y^{-1}, and the lowest erosion rate was 1.86 t h^{-1} y^{-1}.

The large difference in erosion rates in the Tikur Woha catchment between this study and the study of Wolka *et al.* (2015) can be explained by the land cover. Land cover is one of the most important factor in controlling the erosion rate, which is also indicated in this study. Large areas with relative large slope and protective land cover like forest show lower erosion values than more gentle sloped area with seasonal crops. In the study of Wolka *et al.* (2015), the land cover effect is indirectly estimated based on NDVI values derived from unknown satellite image. The final erosion map is dominated by topography; the protective effect of land cover is less visible. It has to be noted that the area in the south east may have much land cover of khat and enset, which can also explain the lower erosion values in this area.

The highest erosion rates are found in areas with the annual crops maize and green beans, especially in the northern part of the study area. During the interview, this area was also indicated as most prone to soil erosion. This can be explained by the fact that land is protected by vegetation only a part of the year. Furthermore, the area is characterised moderate slope and Andosols, which is a soil type that is relative sensitive to soil erosion. The high average erosion values of sugarcane are mainly caused by higher erosion rates on steeper slopes and surface runoff in the north eastern part of the study area. The areas with the highest erosion rates show similar spatial patterns as found in the studies of MoWR (2010) and Ali & Hagos (2016).

5.4 Erosion scenarios

The largest decrease in soil erosion can be found in the reference scenario. Almost the whole study area experienced less than 2.5 t h^{-1} y^{-1}. The two areas with slightly higher erosion rates are both located in the wetland area (appendix 3C). The higher erosion rates in the southern location can be explained by the steeper slopes, and those in the northern location can be explained by the sub basin. In this sub basin, the model estimates the surface runoff based on weather of Koffele, with higher surface runoff because of lower evaporation rates. The higher surface runoff and the land cover wetland result in higher erosion values. Because wetlands on steeper slopes are not likely and the northern area is an artefact of the model, both locations do not represent areas with higher erosion rates.

When the reference scenario is excluded, the largest decrease in the two highest soil erosion rate classes are found in both the cash crop scenarios. In the current situation, 4.9% of the study area is exposed to these erosion categories, in the cash crop A scenario these values are decreased to 2.9% and to 1.5% in the cash crop B scenario. The larger decrease in the cash crop B scenario can be explained that smaller amount of cash crops on the steeper slopes. Although the highest erosion classes decrease in the cash crop A scenario, the average erosion rate increased. A large part of the erosion is located on steep slopes with khat cover. The replacement of protective land cover classes like forest and three plantations with khat explain the higher erosion rates in these areas. In the cash crop B scenario, where only cultivated land is replaced with khat, erosion rates are lower. The erosion rates for the cash crop sugarcane decrease by 30% from 8.6 to 6.1 t h^{-1} y^{-1} in both cash crop scenarios. The effect of the cash crop khat are smaller. In the cash crop A scenario, the increase of erosion is 10%, while in the cash crop B scenario the decrease of erosion is 3%. An explanation for the smaller change is that sugarcane mainly replaces maize and beans with high erosion rates, khat on the other hand replaces both land covers with higher and lower erosion rates for example agricultural crops and forest.

In the policy scenario, the khat on steep slopes is replaced with forest. The total average erosion in the catchment decreased with 0.31 t h^{-1} y^{-1} (7 %). The total average erosion of khat decreased with 22% from 4.2 to 3.3 t h^{-1} y^{-1}, the erosion rate of forest area doubled from 0.02 to 0.04 t h^{-1} y^{-1}. Although the overall erosion decreases, the areas with high erosion rates (>15 t h^{-1} y^{-1}) are not effected in this scenario. The main change in erosion rates is found in areas with moderate and low erosion rates (<15 t h^{-1} y^{-1}).

In all scenarios mentioned above, khat has a negative effect on soil erosion, except from the cash crop B scenario which show a small positive effect. The current land cover change trend shows that both food crops and forest are converted to khat (Dessie & Kinlund*,* 2008). Therefore, it is likely that the khat expansion in the Tikur Woha catchment will have a negative effect on erosion, although the erosion rates increased not for the area with higher erosion rates (>15 t h^{-1} y^{-1}).

The SWC measures resulted in decrease of 25% of average erosion in the total catchment and a decrease of 27% on the cultivated crops. Beside the reference scenario, the SWC scenario is the most effective in reducing soil erosion rates. The reduction of soil erosion rates is similar to the reduction of 10-50% found by Temesgen *et al.* (2012). Compared to the structural erosion control on cropland of 63% found by Meshesha *et al.* (2012), the reduction of soil erosion is lower. Compared to the policy scenario, soil erosion rates are more effectively reduced in the SWC scenario. Both the average erosion rates and the two highest erosion rates classes are reduced more. The policy scenario is only more effective in reducing soil erosion rates in the south eastern part of the study area, which is characterised by a relative high percentage of khat cover and steeper slopes.

6 CONCLUSION AND RECOMMENDATIONS

The current land cover in the Tikur Woha is dominated by cultivated land. The dominant land cover in the catchment are khat, maize and enset. With the current land cover, average soil erosion rates are relatively low (4.32 t h^{-1} y^{-1}). Only a small part (<5%) is the Tikur Woha catchment is exposed to higher erosion rates (>15 t h^{-1} y^{-1}). Higher erosion rates area mainly found on steeper soils (>30%) with cultivated crops such as beans, teff, and sugarcane. Despite the relatively low erosion rates, the erosion increased compared to the simplified natural situation of the reference scenario (0.12 t h^{-1} y^{-1}). Except form the cash crop A scenario, a reduction of the average soil erosion rates is observed for all land cover changes and soil conservation practice (tillage). Besides the reduction in average soil erosion rates in most scenarios, the soil erosion rates above 15 t h^{-1} y^{-1} did not increase for all scenarios. Given current land cover trends, it is likely that the cash crops like khat and sugarcane will increase in the future. If the current trend continues and both natural vegetation like forest and cultivated land are replaced with cash crops, average erosion rates will increase. However, when only agricultural land is replaced with cash crops a decrease in erosion rates is shown. From a policy side, it is more effective to implement SWC measures than to replace khat with forest on steeper slopes, when considering average soil erosion rates. Although average soil erosion rates for the total catchment are relatively low, there are areas with higher erosion rates, mainly steeps slopes with cultivated land. Therefore, policy maker should focus on the implementation of soil and water conservation and maintaining and restoring natural vegetation in these areas to reduce soil erosion rates in the future.

Further research could focus on the effect on different soil and water conservation measurement in these areas in combination with restoring of natural vegetation. These scenarios showed the largest reduction in soil erosion rates for the most sub basins. In areas with higher erosion rates in the soil and water conservation scenarios, replacement of natural forest should be investigated. In this study, it is shown that erosion rates show large variation between wetter and dryer years. To be able to make better estimates of future erosion rates, future research could incorporate the effect of climate change on soil erosion rates. Furthermore, model results could improve by correcting crop parameters for the local environment and by adding missing plant types such as khat and enset to the database. This will likely result in better erosion estimates because land cover is one of the most important factors that influence soil erosion rates.

REFERENCES

Ali, S. A., & Hagos, H. (2016). Estimation of soil erosion using USLE and GIS in Awassa Catchment, Rift valley, Central Ethiopia. *Geoderma Regional*,*7*(2), 159-166.

Anderson, J. R. (1976). *A land use and land cover classification system for use with remote sensor data* (Vol. 964). US Government Printing Office.

Baatz, M., & Schäpe, A. (2000). J. Strobl, T. Blaschke, G. Griesebner (Eds.). Multiresolution segmentation: an optimization approach for high quality multi-scale image segmentation. *Angewandte Geographische Informationsverarbeitung XII*, *58*, 12-23.

Berry, L. (2003). Land degradation in Ethiopia: Its extent and impact. *Commissioned by the GM with WB support*.

Betrie, G. D., Mohamed, Y. A., Griensven, A. V., & Srinivasan, R. (2011). Sediment management modelling in the Blue Nile Basin using SWAT model. *Hydrology and Earth System Sciences*, *15*(3), 807-818.

Bewket, W., & Teferi, E. (2009). Assessment of soil erosion hazard and prioritization for treatment at the watershed level: case study in the Chemoga watershed, Blue Nile Basin, Ethiopia. *Land Degradation & Development*, *20*(6), 609-622.

Boardman, J. (2006). Soil erosion science: Reflections on the limitations of current approaches. *Catena*, *68*(2), 73-86.

Blanco-Canqui, H., & Lal, R. (2008). *Principles of soil conservation and management*. Springer Science & Business Media.

Blaschke, T. (2010). Object-based image analysis for remote sensing. *ISPRS journal of photogrammetry and remote sensing*, *65*(1), 2-16.

Breiman, L. (2001). Random forests. *Machine learning*, *45*(1), 5-32.

Castilla, G., & Hay, G. J. (2008). T. Blaschke, S. Lang, G. Hay (Eds.), Image objects and geographic objects. *Object-based image analysis*,, Springer, Heidelberg, Berlin, New York (2008), pp. 91–110

Congalton, R. G. (1991). A review of assessing the accuracy of classifications of remotely sensed data. *Remote sensing of environment*,*37*(1), 35-46.

Dessie, G., & Kleman, J. (2007). Pattern and magnitude of deforestation in the South Central Rift Valley Region of Ethiopia. *Mountain research and development*, 27(2), 162-168.

Dessie, G., & Kinlund, P. (2008). Khat expansion and forest decline in Wondo Genet, Ethiopia. *Geografiska Annaler: Series B, Human Geography*, *90*(2), 187-203

Diaz-Uriarte, R., 2007. GeneSrF and varSelRF: a web-based tool and R package for gene selection and classification using random forest. BMC Bioinformatics 8.

Dijk, M. van, (unpublished), will be available on *www.studenttheses.library.uu.nl*

Globalweather, 2012. NCEP Climate Forecast System Reanalysis (CFRS). http://globalweather.tamu.edu/, accessed June 2016

Haralick, R., Shanmugam, K., Dinstein, I., 1973. Textural features for image classification. *IEEE Trans. on Systems, Man and Cybernetic*s SMC-3, 610-621.

Hurni, H. (1988). Degradation and conservation of the resources in the Ethiopian highlands. *Mountain research and development*, 123-130.

Hurni, H., & Pimentel, D. (1993). Land degradation, famine, and land resource scenarios in Ethiopia. *World soil erosion and conservation*., 27-61.

Laben, C. A., & Brower, B. V. (2000). *U.S. Patent No. 6,011,875*. Washington, DC: U.S. Patent and Trademark Office.

Landis, J. R., & Koch, G. G. (1977). The measurement of observer agreement for categorical data. *Biometrics*, 159-174.

Lai, R. (2001). Soil degradation by erosion. *Land degradation & development*,*12*(6), 519-539

Legesse, D., C. Vallet-Coulomb & F. Gasse, 2004. Analysis of the hydrological response of a tropical terminal lake, Lake Abiyata (Main Ethiopian Rift Valley) to changes in climate and human activities. *Hydrological Process* ,18,487-504.

Lemessa, D. (2001). Khat (Catha edulis): Botany, distribution, cultivation, usage and economics in Ethiopia. *Addis Ababa: United Nations Development Programme, Emergencies Unit for Ethiopia (UNDP-EUE)*.

Meshesha, D. T., Tsunekawa, A., & Tsubo, M. (2010). Continuing land degradation: cause–effect in Ethiopia's Central Rift Valley. *Land Degradation & Development*, *23*(2), 130-143.

Meshesha, D. T., Tsunekawa, A., Tsubo, M., & Haregeweyn, N. (2012b). Dynamics and hotspots of soil erosion and management scenarios of the Central Rift Valley of Ethiopia. *International Journal of Sediment Research*,*27*(1), 84-99.

Mosbahi, M., Benabdallah, S., & Boussema, M. R. (2013). Assessment of soil erosion risk using SWAT model. *Arabian Journal of Geosciences*, *6*(10), 4011-4019.

MoWR (Ministry of Water Resources), 2010. Rift Valley Lakes Basin Integrated Resources Development Master Plan Study Project. Final Report. Halcrow Group Limited and Generation Integrated Rural Development (GIRD) Consultants

Muzein, B. S. (2006). Remote sensing & GIS for land cover/land use change detection and analysis in the semi-natural ecosystems and agriculture landscapes of the central Ethiopian Rift Valley, Institute for World Forestry, University of Hamburg

Muche, F. Y., & Melesse Temesgen, H. (2014). Effects of Conservation Tillage Integrated with ‘Fanya Juus’ Structure on Soil Loss in Northern Ethiopia. *Global Journal of Science Frontier Research*, *14*(7).

Nyssen, J., Poesen, J., Haile, M., Moeyersons, J., & Deckers, J. (2000). Tillage erosion on slopes with soil conservation structures in the Ethiopian highlands. *Soil and Tillage Research*, *57*(3), 115-127.

Nyssen, J., Poesen, J., Moeyersons, J., Deckers, J., Haile, M., & Lang, A. (2004). Human impact on the environment in the Ethiopian and Eritrean highlands—a state of the art. *Earth-Science Reviews*, *64*(3), 273-320.

Rodriguez-Galiano, V. F., Ghimire, B., Rogan, J., Chica-Olmo, M., & Rigol-Sanchez, J. P. (2012). An assessment of the effectiveness of a random forest classifier for land-cover classification. *ISPRS Journal of Photogrammetry and Remote Sensing*, *67*, 93-104.

Salas, E. A. L., Boykin, K. G., & Valdez, R. (2016). Multispectral and Texture Feature Application in Image-Object Analysis of Summer Vegetation in Eastern Tajikistan Pamirs. *Remote Sensing*, *8*(1), 78.

Saxton, K. E., & Rawls, W. J. (2006). Soil water characteristic estimates by texture and organic matter for hydrologic solutions. *Soil Science Society of America Journal*, *70*(5), 1569-1578.

Shewangizaw, D., & Michael, Y. (2010). Assessing the Effect of Land Use Change on the Hydraulic Regime of Lake Awassa. *Nile Basin Water Science and Engineering Journal*, *3*(2), 110-118.

Shiferaw, B., & Holden, S. (1999). Soil erosion and smallholders' conservation decisions in the highlands of Ethiopia. *World development*, *27*(4), 739-752.

Taddese, G. (2001). Land degradation: a challenge to Ethiopia. *Environmental management*, *27*(6), 815-824.

Tibebe, D., & Bewket, W. (2011). Surface runoff and soil erosion estimation using the SWAT model in the Keleta watershed, Ethiopia. *Land Degradation & Development*, *22*(6), 551-564.

Tamene, L., & Vlek, P. L. G. (2007). Assessing the potential of changing land use for reducing soil erosion and sediment yield of catchments: a case study in the highlands of northern Ethiopia. *Soil Use and Management*, *23*(1), 82-91.

Tamene, L., & Vlek, P. L. (2008). Soil erosion studies in northern Ethiopia. *Land use and soil resources*, 73-100

Temesgen, M., Uhlenbrook, S., Simane, B., Zaag, P. V. D., Mohamed, Y., Wenninger, J., & Savenije, H. H. G. (2012). Impacts of conservation tillage on the hydrological and agronomic performance of Fanya juus in the upper Blue Nile (Abbay) river basin. *Hydrology and Earth System Sciences*, *16*(12), 4725-4735.

Tesfahunegn, G. B., Vlek, P. L., & Tamene, L. (2012). Management strategies for reducing soil degradation through modeling in a GIS environment in northern Ethiopia catchment. *Nutrient Cycling in Agroecosystems*, *92*(3), 255-272.

Trimble, 2011. eCognition Developer 8.64.1 Reference Book. Trimble Germany Documentation, Munchen, Germany, 390

Vogels, M.F.A., Addink, E.A., Jong, S.M. de. (unpublished), Agricultural cropland mapping on black and white aerial imagery using Object-Based Image Analysis and Random Forests

Williams, J. R. (1975). Sediment-yield prediction with universal equation using runoff energy factor. *Present and Prospective Technology for Predicting Sediment Yield*,244-252

Wischmeier, W.H. , Smith, D.D. (1978). Predicting rainfall erosion losses. A guide to conservation planning, United States Department of Agriculture, Washington, D.C..

Wolka, K. (2014). Effect of Soil and Water Conservation Measures and Challenges for its Adoption: Ethiopia in Focus. *Journal of Environmental Science and Technology*, *7*(4), 185-199.

Wolka, W., Tefera, M., Habitamu, T., & Alemayehu, T. (2014). Impact of land cover change on water quality and stream flow in lake Hawassa watershed of Ethiopia. *Agricultural Sciences*, *5*(08), 647.

Wolka, W., Tadesse, H., Garedew, E., & Yimer, F. (2015). Soil erosion risk assessment in the Chaleleka wetland watershed, Central Rift Valley of Ethiopia. *Environmental Systems Research*, *4*(1), 1-12. 29

Wondrade, N., Dick, Ø. B., & Tveite, H. (2014). GIS based mapping of land cover changes utilizing multi-temporal remotely sensed image data in Lake Hawassa Watershed, Ethiopia. *Environmental monitoring and assessment*,*186*(3), 1765-1780

1A: Land cover classification Pleiades

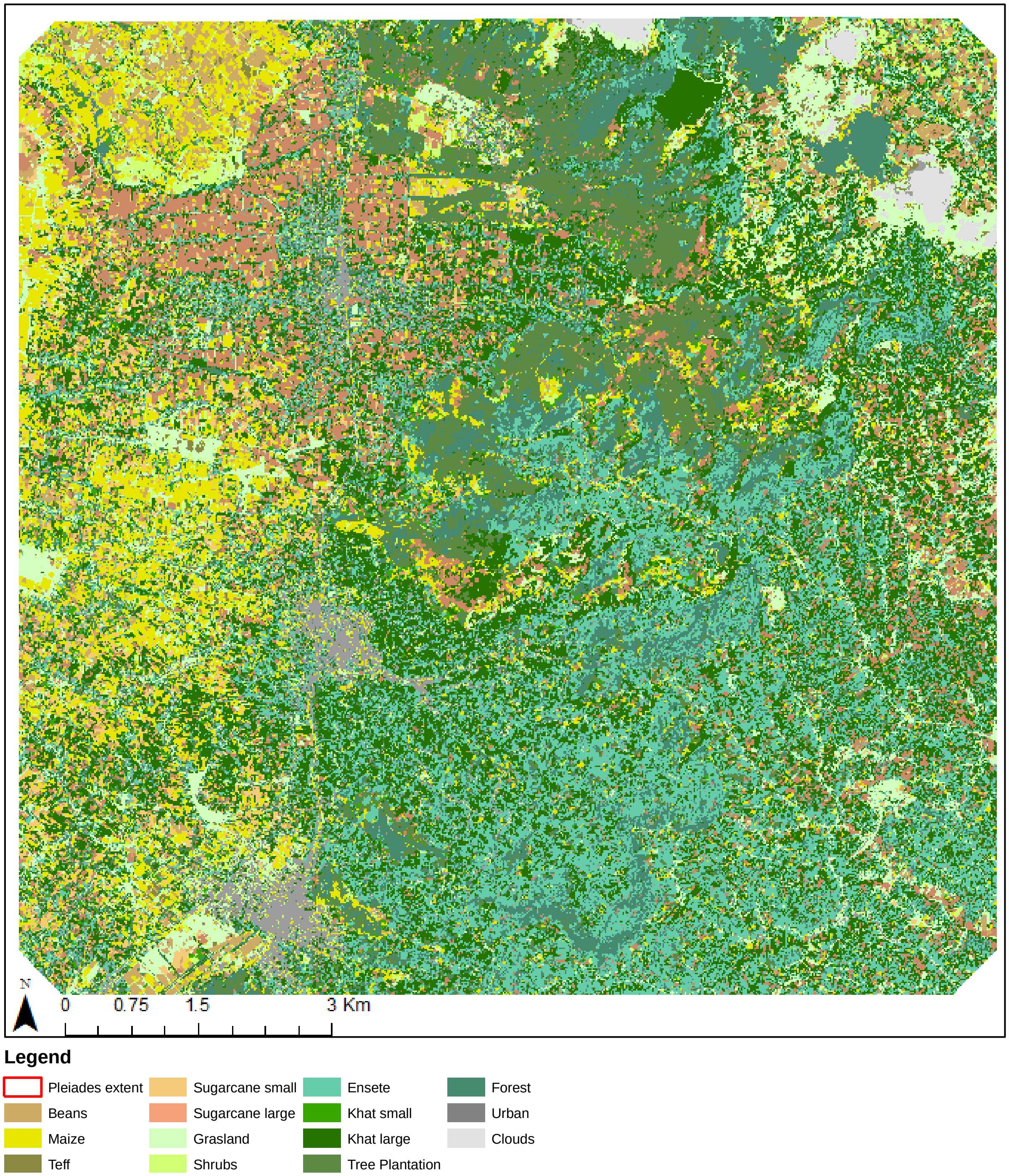

1B: Land cover classification Landsat 8

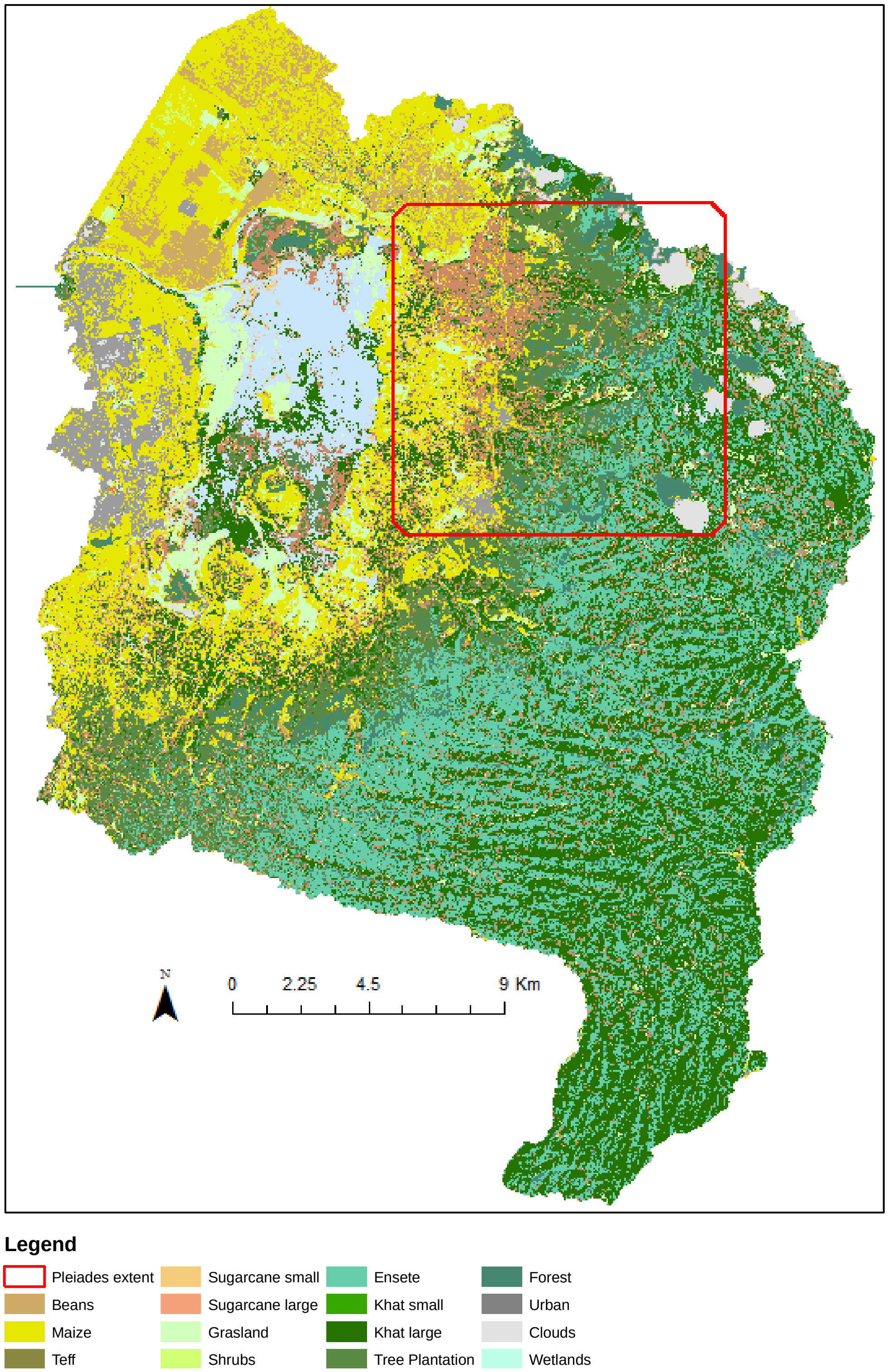

1C: Current land cover based on Pleiades and Landsat 8

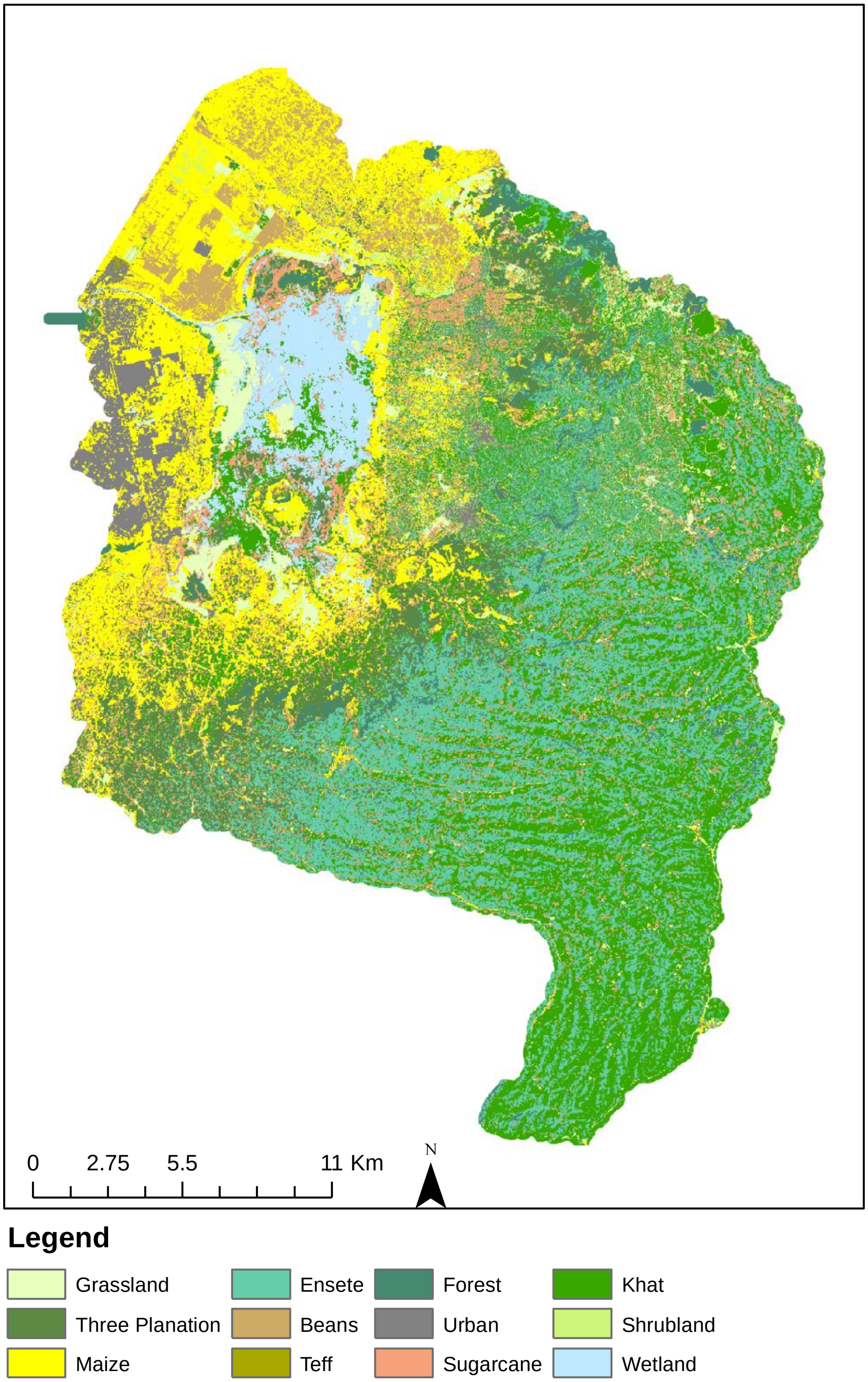

2A: Confusion matrix of the Pleiades classification

Test \ Validation	Grass	Tree plant.	Mais	Enset	Beans	Teff	Forest	Urban	Cloud	Sugarcane	Khat	Shrubs	User’s accuracy	Total
Grass	15	1	0	0	1	3	0	0	0	1	0	2	0.65	23
Tree plant.	0	15	0	2	0	0	0	0	0	0	0	0	0.88	17
Mais	0	0	28	0	4	0	0	0	0	2	0	0	0.82	34
Enset	1	1	0	5	0	0	1	0	0	0	5	0	0.38	13
Beans	0	0	3	0	14	0	0	0	0	1	1	2	0.67	21
Teff	0	0	0	0	0	4	0	0	0	0	0	0	1	4
Forest	0	1	0	0	0	0	9	0	0	1	1	0	0.75	12
Urban	0	0	0	0	0	0	0	16	0	0	0	0	1	16
Cloud	0	0	0	0	0	0	0	0	18	0	0	0	1	18
Sugarcane	2	0	3	0	1	1	0	0	0	28	6	0	0.68	41
Khat	1	0	1	2	0	0	1	0	0	1	17	0	0.74	23
Shrubs	2	1	0	0	0	0	0	1	0	1	0	9	0.64	14
Producer’s accuracy	0.71	0.79	0.8	0.56	0.7	0.5	0.82	0.94	1	0.8	0.57	0.69		
Total	21	19	35	9	20	8	11	17	18	35	30	13		236

2B: Confusion matrix of the Landsat classification

Test / Validation	Grass	Tree Plantation	Maize	Enset	Beans	Teff	Forest	Urban	Cloud	Sugarcane	Khat	Shrubs	Wetlands	User's Accuracy	Total
Grass	189	0	2	0	2	2	0	0	0	1	0	4	2	0.94	202
Tree Plantation	0	815	0	36	0	0	38	0	0	8	5	0	2	0.90	904
Maize	2	1	309	0	31	1	0	0	0	8	1	5	0	0.86	358
Ensete	0	11	0	233	0	0	4	0	0	4	12	1	0	0.88	265
Beans	0	1	19	0	69	0	0	0	0	0	2	0	0	0.76	91
Teff	0	0	0	0	0	1	0	0	0	0	0	0	0	1	1
Forest	0	10	0	6	0	0	270	0	0	0	1	0	0	0.94	288
Urban	0	0	0	0	0	0	0	88	0	0	0	0	0	1	88
Cloud	1	0	0	0	0	0	0	0	98	0	1	0	0	0.98	100
Sugarcane	3	4	2	5	3	0	0	0	0	324	16	1	0	0.91	358
Khat	1	1	1	18	0	0	0	0	0	18	438	0	2	0.91	479
Shrubs	2	0	2	0	1	0	0	0	0	0	0	30	0	0.86	35
Wetlands	1	0	0	0	0	0	0	0	0	0	6	0	112	0.94	119
Producer's accuracy	0.95	0.97	0.92	0.78	0.65	0.25	0.87	1	1	0.89	0.91	0.73	0.95		
Total	199	844	335	298	106	4	312	88	98	363	482	41	118		3288

3A: Average soil erosion over the period 2005-2010 for the cash crop A scenario

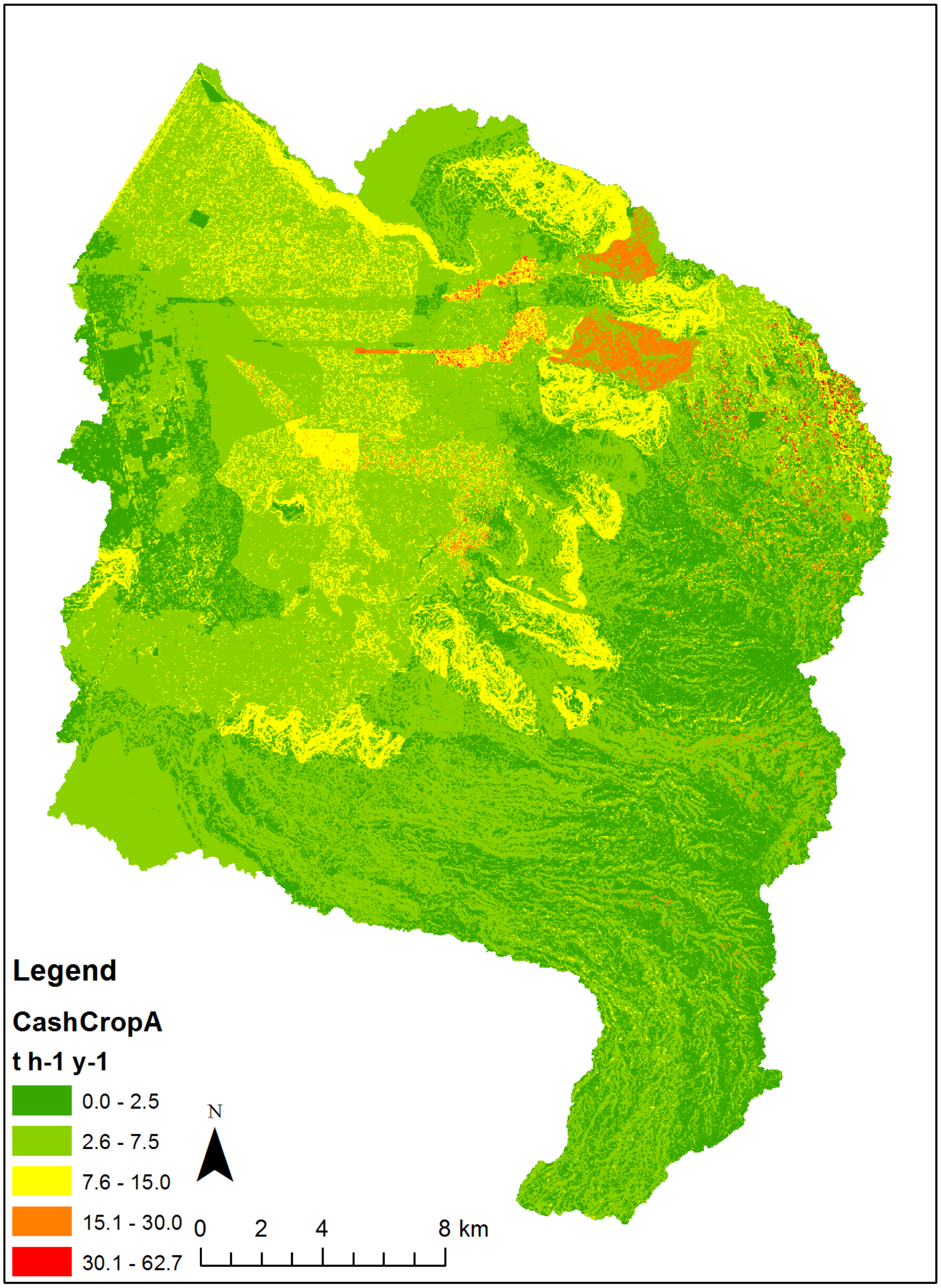

3B: Average soil erosion over the period 2005-2010 for the cash crop B scenario

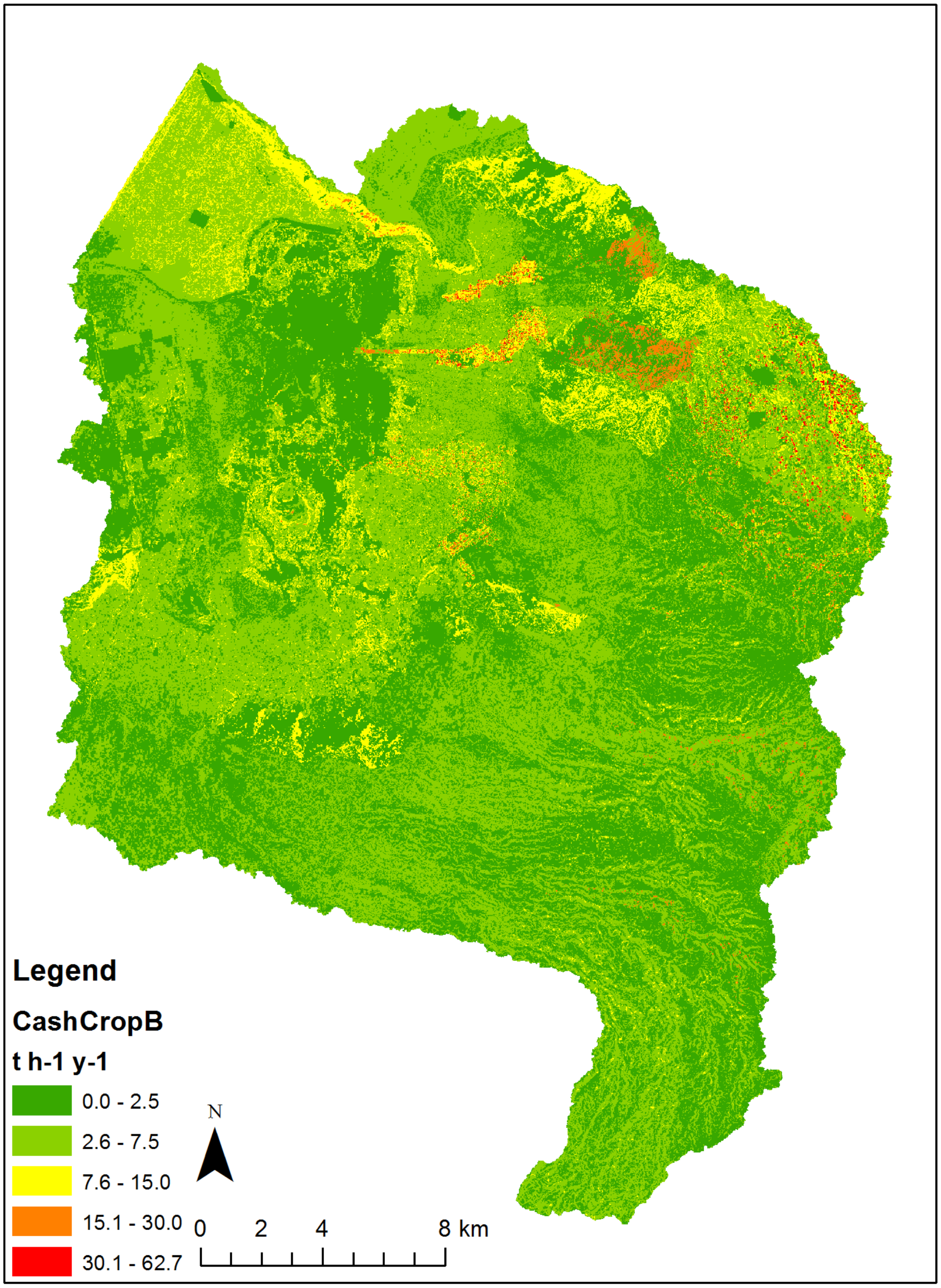

3C: Average soil erosion over the period 2005-2010 for the reference scenario

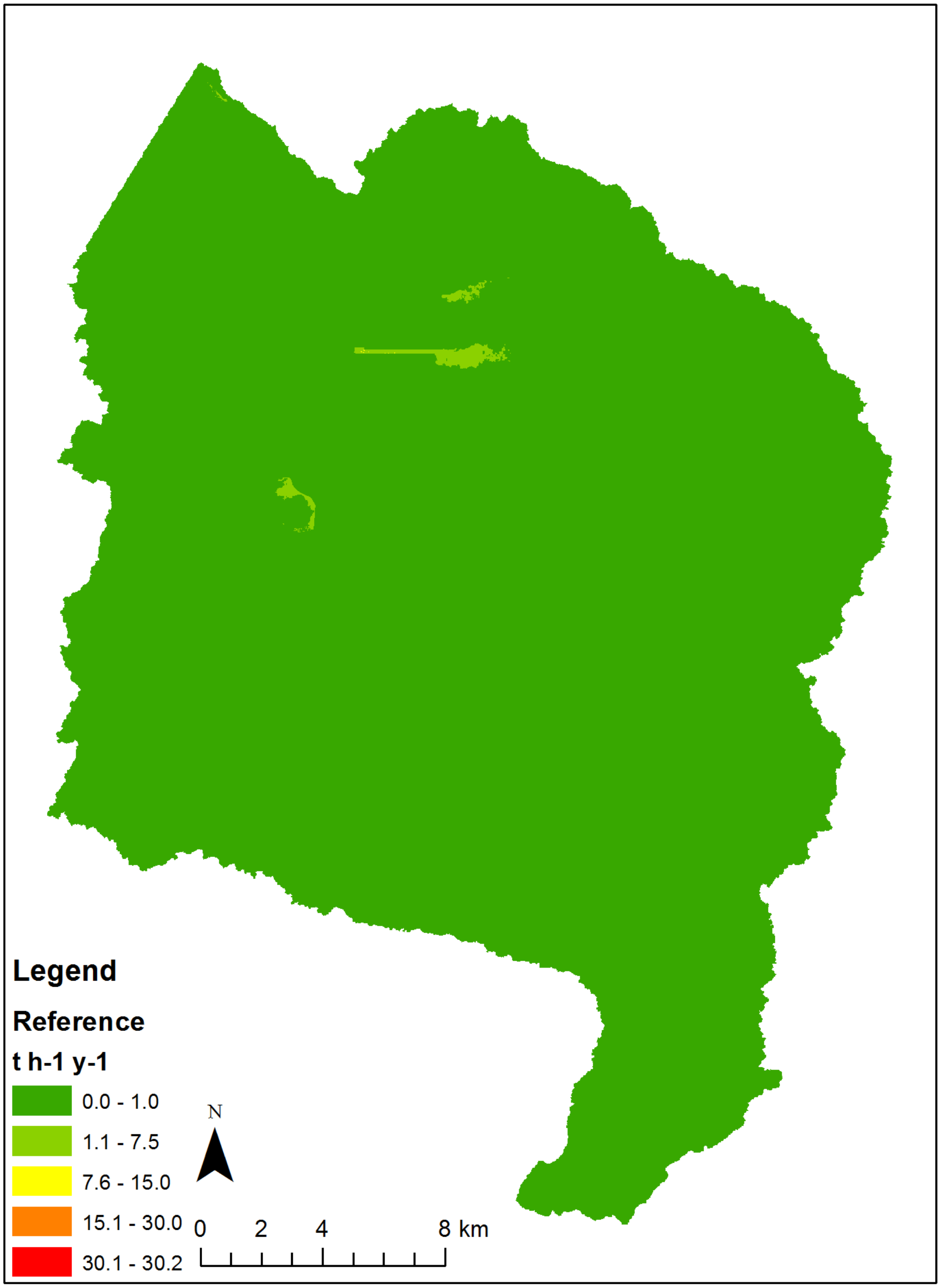

3D Average soil erosion over the period 2005-2010 for the policy scenario

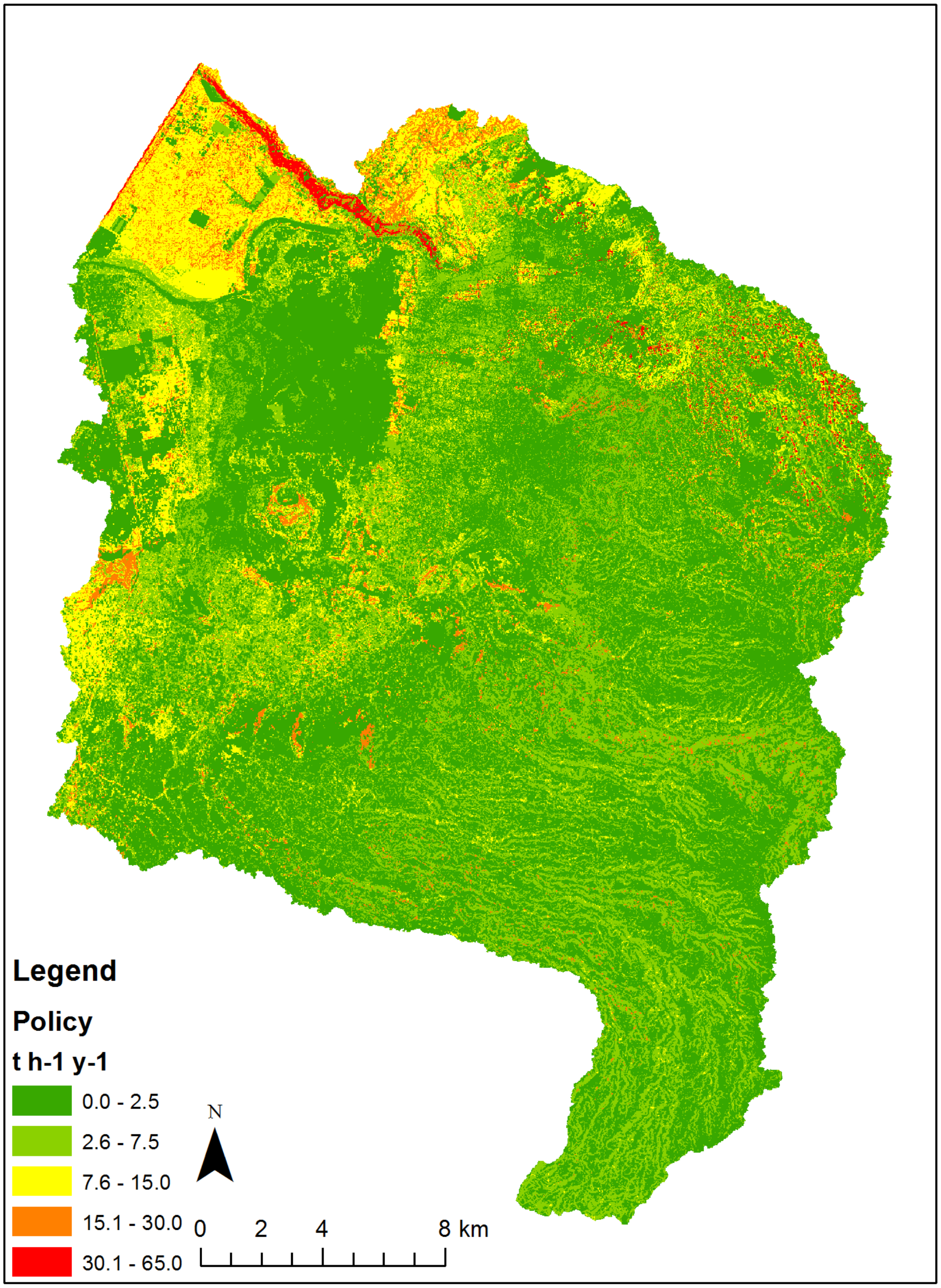

3E: Average soil erosion over the period 2005-2010 for the soil and water conservation scenario